Weierstraß-Institut
für Angewandte Analysis und Stochastik
Leibniz-Institut im Forschungsverbund Berlin e. V.

Preprint ISSN 2198-5855

Coherent passive mode-locking in lasers: Qualitative analysis and numerical simulations

Rostislav M. Arkhipov[1], Ihar Babushkin[2], Mikhail V. Arkhipov[3]

submitted: October 7, 2014

[1] Weierstrass Institute
Mohrenstr. 39
10117 Berlin, Germany
E-Mail: Rostislav.Arkhipov@wias-berlin.de

[2] Institut für Quantenoptik
Universität Hannover
Welfengarten 1
30167 Hannover, Germany
E-Mail: babushkin@iqo.uni-hannover.de

[3] Faculty of Physics
St. Petersburg State University
Ulyanovskaya 1 Petrodvoretz
198504 St. Petersburg, Russia
E-Mail: m.arkhipov@spbu.ru

No. 2019
Berlin 2014

2008 *Physics and Astronomy Classification Scheme.* 42.60.Fc, 42.65.Re, 42.50.Md, 42.60.Da .

Key words and phrases. mode-locking, ultrashort laser pulse, coherent pulse propagation, area theorem, self-induced transparency.

R. M. Arkhipov would like to acknowledge the support of EU FP7 ITN PROPHET, Grant No. 264687.

Edited by
Weierstraß-Institut für Angewandte Analysis und Stochastik (WIAS)
Leibniz-Institut im Forschungsverbund Berlin e. V.
Mohrenstraße 39
10117 Berlin
Germany

Fax: +49 30 20372-303
E-Mail: preprint@wias-berlin.de
World Wide Web: http://www.wias-berlin.de/

Abstract

In the present work we report the possibility of passive mode-locking based on the coherent interaction of light with the amplifying and absorbing media in lasers with ring and linear cavities. We consider the realistic and practically interesting case when the absorbing and amplifying media are separated in the cavity space but not homogeneously mixed in the volume of the cavity, as was considered earlier in the literature. We perform qualitative consideration of coherent passive mode-locking based on the area theorem of McCall and Hahn and its graphical representation for the first time. We show that other, not soliton scenarios of passive mode-locking exist, and that coherent mode-locking is self-starting (lasing without an injection seeding pulse is possible). We point to the fact that the spectral width of the laser generation can be significantly larger than the spectral bandwidth of the gain medium. Numerical simulations were performed using the system of Maxwell-Bloch equations in the slowly varying envelope approximation.

1 Passive mode-locking in lasers, basic theoretical approaches

Investigations of mode-locking in lasers began as soon as the first lasers were developed in the 1960s [1–7]. As we mentioned in the introduction, discovering mode-locking led to a great success in the realization of extremely short laser pulses with high peak power. Below we consider the basic approaches that are used to describe theoretically passive mode-locking regimes in lasers.

The primary element allowing periodic pulse generation is the nonlinear absorber. A nonlinear absorber is a material where the absorption decreases with increase of the light intensity. Such materials as dyes, crystals or semiconductors with strong resonant absorption can be used for this purpose. The latter are most actively used nowadays, because of their significant advantages in comparison to dye absorbers and other solid state materials used before (see Refs. [8–12]). As an example of the recent progress in this area, the discovery of so-called semiconductor saturable absorber mirror (SESAM) [8, 13] can be mentioned. In this device, semiconductor absorber material is integrated into the laser mirror which results in dependence of the mirror reflectivity on the light intensity. Such a technique allows for the creation of passively mode-locked solid state lasers generating light pulses with a duration from femtoseconds to nanoseconds [8, 13].

Passive mode-locked semiconductor lasers are actively studied today. In such lasers, quantum dot and quantum well materials can be used for both gain and absorbing sections, resulting in short optical pulses with a repetition rate in the range from few to hundreds GHz [9–12, 14]. Due to their compact size and high repetition rate they are considered as promising candidates for optical communication systems.

Before the detailed discussion of theoretical approaches to passive mode-locking mechanism, an important remark is to be mentioned. Short pulse propagation occurring in a resonant medium strongly depends on the ratio between the two parameters: pulse duration τ_p and polarization relaxation time T_2. There are two general situations that can be imagined in this context, typically referred to as an incoherent interaction of a light pulse with medium, and the coherent interaction [15–17]. In the former case the pulse duration is much larger than the polarization relaxation time, $\tau_p >> T_2$. Polarization of the medium "follows"the optical field in a quasi-stationary manner and can be adiabatically eliminated from the model equations describing interaction of the light with medium [15, 17]. During the pulse propagation, it reduces the population difference in the medium, thus making it saturated. Therefore, the term “saturable” is used in the literature to denote such absorber. Due to the lack of instantaneous nontrivial dynamics of the atomic polarization, such type of mode-locking will be called “incoherent” in the following, in contrast to “coherent” mode-locking considered below. The majority of the papers considering theoretically passive mode-locking are based on an incoherent approximation. We briefly overview this class of theories.

P. G. Kryukov and V. S. Letokhov explained mode-locking using so-called fluctuation mechanism [18–21]. According to this model the laser radiation at the low-intensity linear stage contains a lot of chaotic ultrashort spikes. At the next, nonlinear, stage, when the intensity of radiation increases, the absorbing medium bleaches. This leads to a faster amplification of the spikes having the highest intensity, and, simultaneously, to their compression. Thus, a periodic sequence of mode-locked ultrashort pulses appears. This model was successfully applied to an explanation of mode-locking regimes in Ruby, Nd-glass and other lasers.

Analytical study of passive mode-locking was first performed by H. Haus, see Refs. [22, 23] and review [24]. His theory was developed for so-called fast and slow saturable absorbers and contains significant simplifications. In the case of fast saturable absorber (see Ref. [23]) its population difference relaxation time must be much smaller than the pulse duration. Another simplification is that the pulse shape does not change significantly per cavity round-trip and that the absorber saturation is relatively weak. In Ref. [22] an analytical study of passive mode-locking with so-called slow saturable absorber was performed. In this theory the pulse duration is assumed to be much smaller than the absorber recovery time. Besides, the approximation of a weak gain and absorption were assumed. In Ref. [25] New also developed an analytical theory of mode-locking. He demonstrated that combined action of the absorption and saturation in the amplifier can lead to a pulse compression. The results obtained by New were applied to explain the picosecond pulse generation in mode-locked dye lasers. Further development and analysis of the mode-locking models were performed in Refs. [26–28]. This analysis was based mainly on the numerical simulations.

The disadvantages of the Haus and New approaches were elucidated in Refs. [29–31]. In particular, the ability of the models of Haus and New to adequately describe real laser systems were questioned for many practical situations. For example, semiconductor mode-locked lasers have rather high gain and losses per cavity round-trip. To overcome this limitation, in Refs. [29–31] a delay differential equations (DDE) model was developed. This model is able to describe mode-locking in the parameter range typical for semiconductor lasers. The only essential assumption of this model was a ring-cavity geometry with unidirectional lasing. An analytical and numerical

study of such a model is possible using bifurcation analysis and asymptotic techniques. Furthermore, the DDE model and some its generalizations were successfully applied to study different dynamical regimes in passively mode-locked lasers [31–36].

Let us consider a qualitative physical picture of the pulse evolution in a mode-locked laser [15, 37]. After the pulse passes through the absorber, its leading edge is strongly attenuated. On the other hand, the trailing edge propagates in the medium which is already saturated and thus experiences weaker absorption rate. As a result, the laser pulse shape becomes asymmetric, see Fig. 1a. Note that the pulse maximum is shifted backward during this process, meaning that it moves at a velocity smaller than the velocity of light in vacuum c.

In the amplifying medium the situation changes significantly. The pulse front propagates in a still unsaturated medium and thus is strongly amplified. The gain becomes saturated, and the trailing edge grows slower, as illustrated in Fig. 1b. As a result of nonlinear amplification, the pulse maximum is shifted forward. Therefore, the velocity of the pulse maximum is larger than the light velocity in vacuum c. This, of course, does not contradict the causality principle. The possibility of superluminal propagation of the pulse maxima in an amplifying medium was demonstrated experimentally and theoretically in Refs. [15, 38–41]. As a result of this process the resulting pulse is narrowed and achieves its stationary shape after many round-trips. This process is illustrated in Fig. 2.

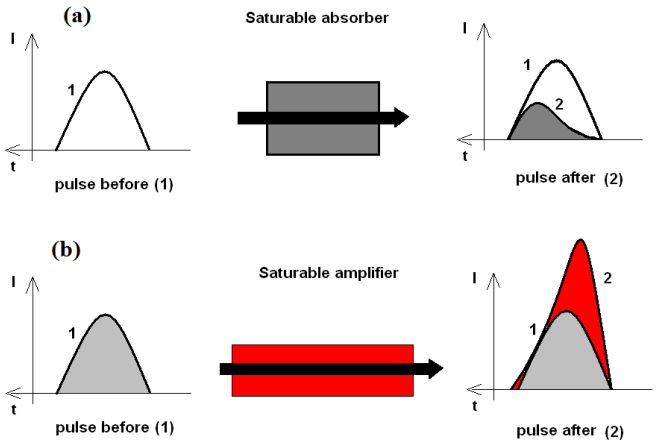

Figure 1: Illustration of the pulse shape evolution in a saturable absorber (a) or saturable amplifier (b) [15, 37].

In contrast to previous considerations, if the pulse duration is short enough, the dipole moment (medium polarization) induced in the nonlinear medium does not have time to decay during the interaction time. This happens if the pulse duration τ_p is much less than the polarization relaxation time, $\tau_p << T_2$, i.e. “coherent” interaction of light with a medium takes place. In this case the polarization of the medium is determined by the field values in the previous time moments and does not “follow” the field, as in the case of incoherent interaction. In other words, the medium possesses a “phase memory” during the relaxation time T_2, which strongly changes the picture of the pulse propagation.

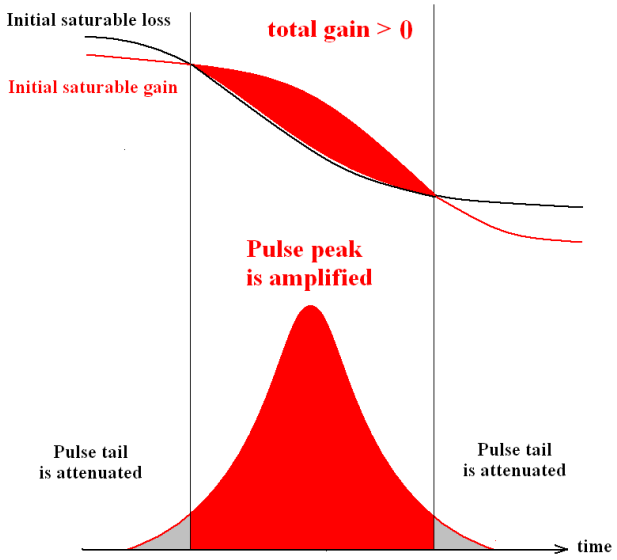

Figure 2: Pulse-shortening process by simultaneous action of the absorber and amplifier [37].

Coherent pulse propagation in amplifying and absorbing media is well-studied currently, see Refs. [15, 16, 42–52]. In the case of such coherent interaction, an interesting phenomenon of self-induced transparency (SIT) may arise. SIT was discovered by S. L. McCall, E. L. Hahn in Refs. [42, 43] and observed experimentally in different media. The influence of SIT on the pulse propagation is the following: the leading edge of the pulse transfers the particles from the ground energy state to a coherent superposition of the ground and excited states. Thus, some part of the field energy is stored in the medium. The trailing edge of the pulse causes the atoms to emit electric field and thus the energy stored in the medium returns back to the field. In this way, the atoms are excited at the leading edge of the pulse and move back to the ground state at the trailing edge. In this way, the pulse may restore its initial shape during the propagation and thus travel in the nonlinear medium without loss of energy. This leads, however, to the decrease of the pulse velocity. The important quantity describing the pulse dynamics in the coherent regime is the pulse area, defined as [43]:

$$\Phi(t,z) = \frac{d_{12}}{\hbar}\int_{-\infty}^{t} \mathcal{E}(t',z)dt', \tag{1}$$

where d_{12} is the transition dipole moment of the two-level atom, and $\mathcal{E}(t,z)$ is the pulse envelope. The area Φ of a stable SIT-induced soliton is 2π. An important result of the SIT theory is the so-called pulse area theorem. This theorem governs the evolution of the pulse area Φ during its propagation in a two-level absorbing (or amplifying) medium with an inhomogeneity broadened line [15, 16, 43, 44]:

$$\frac{d\Phi}{dz} = -\frac{\alpha_0}{2}\sin\Phi, \tag{2}$$

where

$$\alpha_0 = \frac{8\pi^2 N_0 d_{12}^2 \omega_{12} T_2^*}{\hbar c}, \tag{3}$$

is the absorption coefficient per unit length, N_0 is the concentration of two-level atoms, ω_{12} is the medium transition frequency and $1/T_2^*$ is the width of inhomogeneously broadened line. The solution of (2) is

$$\tan(\Phi/2) = \tan(\Phi_0/2)e^{-\alpha_0 z/2}, \tag{4}$$

where Φ_0 is the initial pulse area. The solution of (2) is presented in Fig. 3a. According to Fig. 3 the area of pulses with Φ_0 smaller than π tends toward 0 during propagation in the medium (see also Fig. 3b). If the pulse area is slightly larger than π (for example $\Phi_0 = 1.1\pi$ as in Fig. 3a), the pulse area tends to a stationary value 2π and a stable soliton is formed. Besides, the pulse duration increases simultaneously, see Fig. 3c. In contrast, if the initial pulse area $2\pi < \Phi_0 < 3\pi$ as in Fig. 3d, pulse narrowing takes place. And finally, if the Φ_0 close to 4π initial pulse may split into 2 separate 2π pulses, see Fig. 3e, where the evolution of pulse shape for $\Phi_0 = 3.6\pi$ is illustrated.

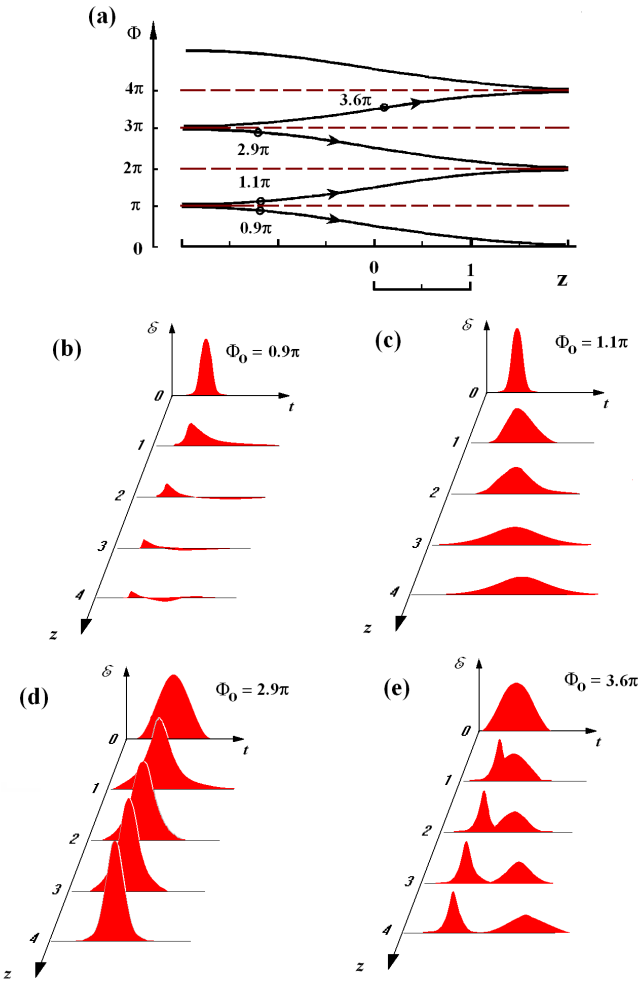

Figure 3: (a) Branches of solution of Eq. (2). For an absorbing (amplifying) medium with $\alpha_0 > 0$ ($\alpha_0 < 0$), the pulse area evolves in the direction of increasing (decreasing) distance z toward the nearest even (odd) multiple of π. (b)-(d): Evolution of pulses with the initial areas $\Phi_0 = 0.9\pi$, $\Phi_0 = 1.1\pi, 2.9\pi, 3.6\pi$ respectively, with distance and time [43].

Coherent pulse propagation in an amplifying medium can be also described by (2) taking into

account the fact that α_0 changes its sign. From Eq. (2) it follows that the same diagram Fig. 3a can be used, only the opposite z-direction must be taken. Accordingly (see Fig. 3), a pulse with the initial area $\Phi_0 < \pi$ (or 2π) approaches a steady-state with the area π. During this process, the pulse duration decreases. Note that such π-pulse leaves the initially excited two-level atoms in the ground level after its passage.

Thus, a stable 2π soliton in an absorbing medium, and a stable π soliton in a gain medium can be formed. This fact was first noted in Ref. [15] where a coherent pulse propagation in a two-component medium containing a gain and absorbing material was studied theoretically.

This observation led to the proposal of so called coherent passive mode-locking, a theory developed in Refs. [53, 54] and later expanded upon in recent papers [55–59]. In order to achieve 2π and π pulse areas in the absorbing and gain medium respectively, it is necessary to take the dipole moment of the absorbing medium two times larger than the dipole moment of the gain medium. In contrast to the case of usual passive mode-locking, coherent mode-locking allows for the generation of optical pulses with spectral bandwidth larger than the bandwidth of the gain medium. On the other hand, in Refs. [53–59] it was assumed that both the absorbing and amplifying media are homogeneously "mixed" in the same sample. This is difficult to realize for most of passively mode-locked laser systems [9–12, 14], with the exception of a quantum cascade laser structure developed in [55, 56]. Because of this, below in this work we will extend the theoretical analysis of the coherent mode-locking to the case when both absorber and gain medium are placed separately in the cavity.

Before proceeding further with numerical analysis, let us consider the pulse evolution qualitatively, using a drawing showing the evolution of the pulse area in different parts of the cavity, which we refer to as McCall-Hahn diagrams in the following. It allows us for better understanding of basic mechanisms responsible for the pulse generation in a situation when the gain and absorber sections are separated, as well as to estimate the range of parameters where the coherent mode-locking is possible. We note that such an analysis, to the best of our knowledge, have never been considered in the literature before.

2 Area theorem and coherent mode-locking

In this section we present analysis of coherent mode-locking using the graphical representation technique which we call "McCall and Hahn diagrams".

Consider the situation when the absorbing and amplifying media are separated in space and the dipole moment of the absorber is twice that of the amplifier. Let us plot the solutions of Eq. (2) for the absorber and amplifier on the same plane for the case when the coefficient α_0 determined by Eq. (3) is the same for both media (in this case N_0 in the amplifier is four time that of the absorber). The branches of solutions of Eq. (2) placed in this way are shown in Fig. 4. Importantly, we can chose the direction of motion along the branch of the absorber (blue curves noted as $1a$, $2a$, $3a$, $4a$) from left to right, whereas for the amplifier it is opposite, from right to left (red curves noted as $1g$, $2g$), which is explained by the opposite signs of α_0 in both sections.

Using such diagram technique we are able to see immediately the most important peculiarities

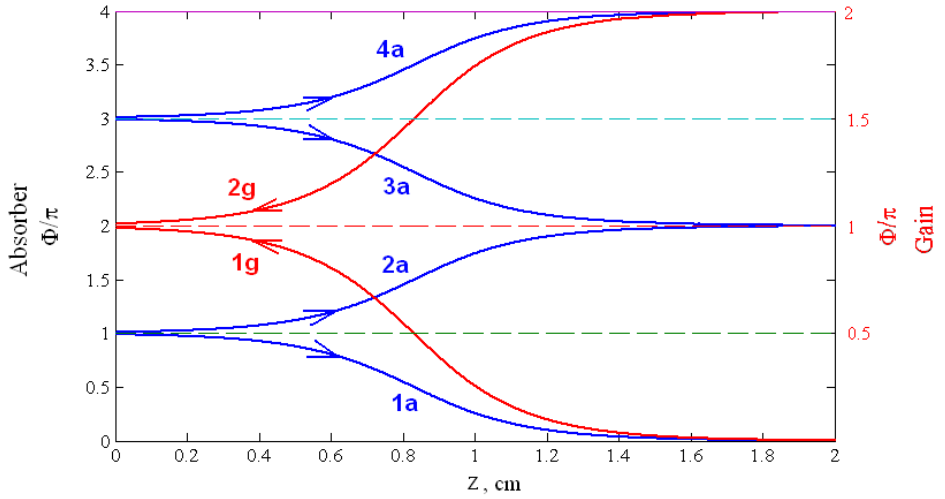

Figure 4: Branches of solution of Eq.(2) for the absorber 1a, 2a, 3a, 4a (blue lines) and the amplifier 1g, 2g (red line) for $|\alpha_0| = 10$ cm^{-1}.

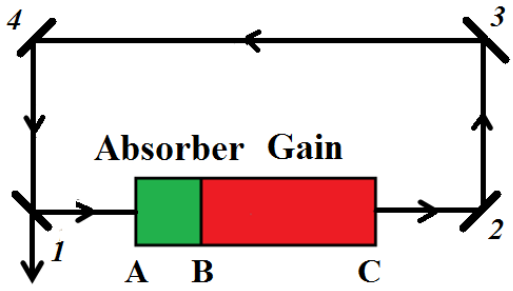

Figure 5: Schematic representation of mode-locked laser with a ring cavity where unidirectional counter clockwise lasing is assumed.

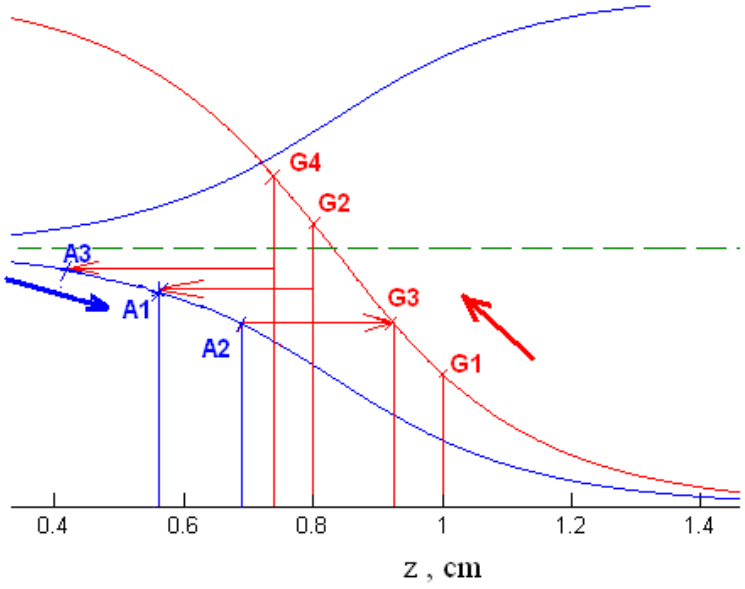

Figure 6: Using the McCall and Hahn diagrams from Fig. 4 for illustration of the pulse area evolution. The pulse evolution follows the path $G1 \to G2 \to A1 \to A2 \to G3 \to G4 \to A3$ in the gain (along red line) and in the absorber (along the blue line) sections in z-direction, backward and forward, correspondingly, which reflects different signs of α in both sections. The vertical sections of the path correspond to the reflection from the mirror, when the pulse area decreases.

of the pulse area evolution. Let us assume that we have a laser with a ring cavity operating in a unidirectional lasing regime, see Fig. 5. In this laser a short pulse satisfying the condition of coherent interaction passes through the amplifier, is reflected from the mirror 1 with the reflection coefficient for the field R, and then enters the absorber. Assume that the other mirrors do not produce any energy loss. We also assume that the pulse travels long enough in every cavity section such that both the gain and absorber are able to recover to their equilibrium values between the pulse passages. Let us now suppose that a short pulse with the initial area $\Phi_0 = 0.25\pi$ enters the amplifier (cf. Fig. 6). This area corresponds to the point $G1$ on the red (amplifier) curve. Propagation in the amplifier corresponds to a shift of this point from right to left along the amplifier branch (red curve in Fig. 6) to $G2$, which is accompanied by an increase of the pulse area. After the pulse passes the amplifier, it is reflected by a non-ideal mirror and its area is thus reduced. Hence, the working point moves down vertically from $G2$ by the distance corresponding to the pulse area decrease caused by the reflection. Then, moving along the straight line parallel to the horizontal axis one arrives to the point $A1$, which now describes the pulse entering the absorber. Evolution of the pulse in the absorber is described by moving from left to right along the blue branch until the point $A2$. Now one returns back to the gain branch in $G3$. The point $G3$ is located above the initial point $G1$, meaning the overall increase of the pulse area after the whole cycle.

Now we repeat the cycle by moving from $G3$ again along the gain curve, arriving to $G4$, then descend down to $A3$ on the absorber curve, and so on. Note that the pulse area increases because the slope of the gain curve (and its length) is larger than that of the absorption curve. Finally, after long run the pulse area at the output of the amplifier and absorber will approach π and 2π, respectively, leading to a stationary pulsating regime. Note that if we decrease the mirror reflection coefficient strongly enough, or, alternatively, increase the absorber length, the working point might now move down every cycle thus tending toward zero, meaning the pulse decay.

Using such an approach one can predict whether a stable limit cycle exists and can be achieved from an initial pulse with the small area. The appearance of such limit cycles can be confirmed by numerical simulations. An example of such cycle and its development is presented in Fig. 7. For the exemplary parameters a regime develops from the initial pulse with the small area $\Phi_0 = 0.001\pi$ in 50 round-trips times as shown in Fig. 7a, which approaches the limit cycle depictured separately in Fig. 7b.

The difference between the slopes of the amplifier and absorber curves allows us to start the iteration process from very small pulse areas and approach finally the nonzero limit cycle. That in particularly means, that an injection of a seed pulse is not always necessary to achieve the stationary short-pulse regime. This is in contrast to the scheme with “mixed” absorber and gain used in previous considerations of coherent mode-locking, where the initial pulse is absolutely necessarily to achieve the pulsed regime.

Nevertheless, if we increase the absorber length, the low-signal limit becomes purely absorbing, thus requiring injection of a seed pulse to start generation. Fig. 7 illustrates this point. In particular, Fig. 8a illustrates the evolution of the pulse area with the absorber length increased 2 times in comparison to that in Fig. 7 and initial pulse area $\Phi_0 = 0.15\pi$. In this case the system tends to zero pulse area. On the other hand, if one starts from $\Phi_0 = 0.2\pi$, the system approaches a

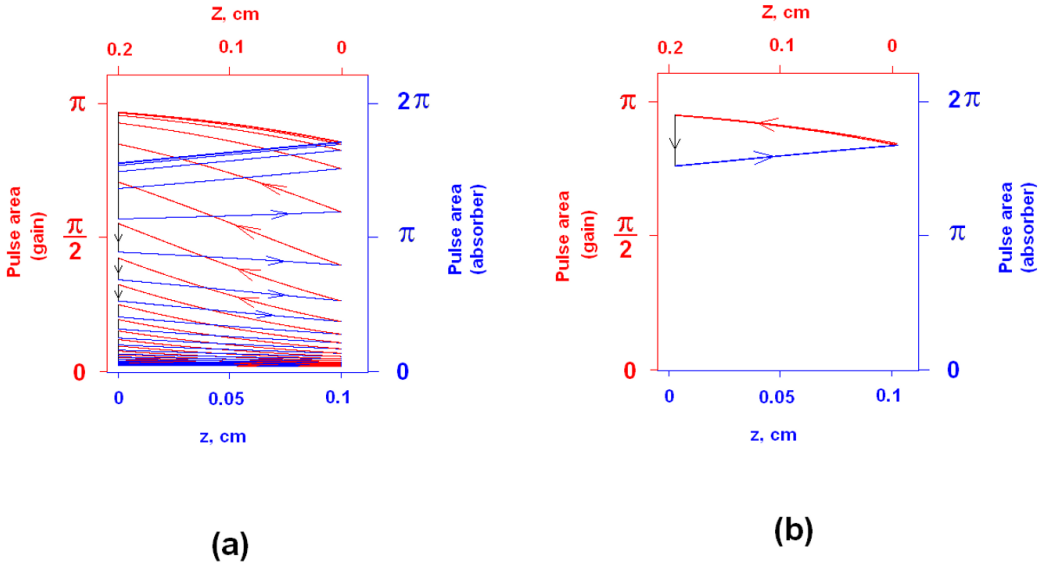

Figure 7: Evolution of the pulse area Φ in the absorber and gain medium (a) from the initial value $\Phi_0 = 0.001\pi$ to a limit cycle (b) in a ring cavity geometry. The blue and red curves corresponds to the pulse propagation in the absorber and gain sections, correspondingly.

nonzero limit cycle after 7 round-trips, as shown in Fig. 8b.

Using the area theorem Eq. (4) one can easily obtain the condition of lasing self-starting for coherent mode-locking. Suppose that the gain and absorber sections have the lengths L_g, L_a and the gain (absorption) coefficients α_{0g} and α_{0a} respectively, and the process starts from a weak pulse with the initial area $\Phi_0 \ll 1$, meaning that the working point is on the lower part of the red branch in Fig. 6. Since in the lower part of the branches $\Phi \ll 1$, $\tan(\Phi) \approx \Phi$, the area theorem Eq. (4) can be rewritten in the form:

$$\Phi \approx \Phi_0 e^{-\alpha_0 z/2}. \tag{5}$$

Assume that a seed pulse with the initial area for gain medium $\Phi_{0B} \ll 1$ starts propagating in the amplifier at the point B, see Fig. 5. At the output of the gain section (point C) the pulse area according to Eq. (5) will be

$$\Phi_C = \Phi_{0B} e^{\alpha_{0g} L_g/2}.$$

Since only the part of the radiation is reflected from the mirror 1, the initial pulse area for absorber (point A in Fig. 5) is given by $\Phi_A = R m_d \Phi_C$, where $m_d = d_{12a}/d_{12g}$ the ratio of absorber/gain dipole moments. After passing through the absorber (point B) the pulse area will be:

$$\Phi_B = \Phi_A e^{-\alpha_{0a} L_a/2} = R m_d \Phi_{0B} e^{\alpha_{0g} L_g/2} e^{-\alpha_{0a} L_a/2}. \tag{6}$$

In order to self-start the lasing one must have $\Phi_B \geq m_d \Phi_{0B}$. This condition can be rewritten in the form:

$$R e^{\alpha_{0g} L_g/2} e^{-\alpha_{0a} L_a/2} \geq 1. \tag{7}$$

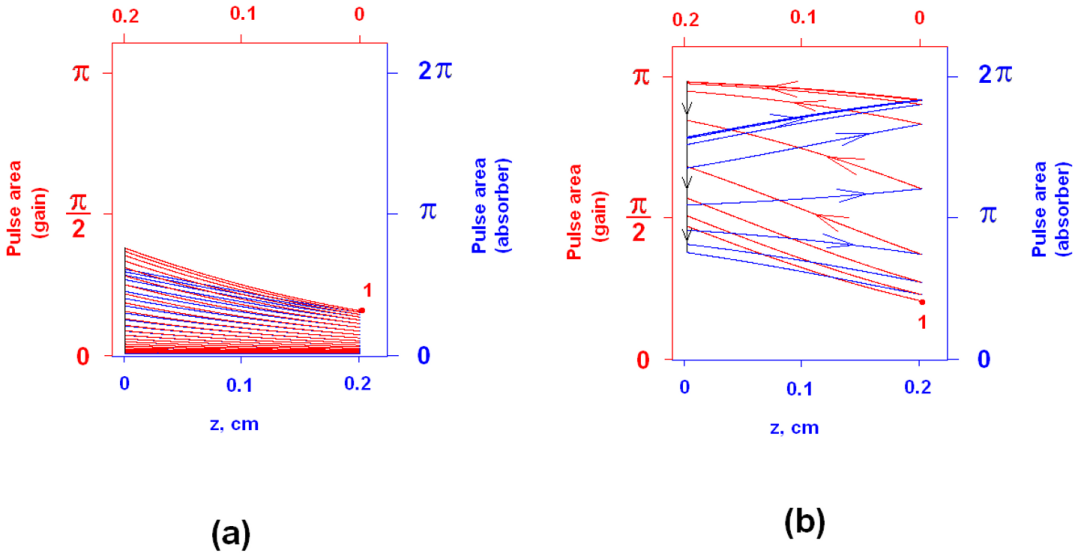

Figure 8: Evolution of the pulse area Φ in the ring cavity geometry for large length of the gain section. The evolution starts from the point 1, which corresponds to $\Phi_0 = 0.15\pi$ in (a) and $\Phi_0 = 0.2\pi$ in (b). In the former case, the system approaches zero, whereas in the later one it moves toward a nonzero limit cycle.

With the help of the diagrams introduced above (and Fig. 3 where the MCall and Hahn solution is illustrated) we will now analyze the situation, when the ratio of the dipole moments is not equal to two. First, we consider the case when $m_d < 1$. The corresponding diagram for $m_d = 0.5$ is shown in Fig. 9a. In this case the limit cycle is realized with the branch $1g$ of the amplifier and $1a$ of the absorber. On the amplifier branch, the pulse with the area tending to π is formed, whereas the absorber will decrease the pulse area. Because of the energy conservation, decrease of the pulse area means that the pulse envelope must change its sign. Thus, the generated pulse must have at least one point of zero intensity. Experimental observation and theoretical study of such zero-area (0π) formation in the absorber medium was presented in [60, 61].

In the example presented in Fig. 9b we set $m_d = 1.5$. In this case, the branch $1g$ of amplifier and one of the branches $1a$ or $2a$ of the absorber can take part in the generation. A limit cycle formed with $1g$ and $2a$ has the following feature: when moving along $2a$, the pulse area tends to 2π and its duration increases in contrast to the cycle with $1g$ and $1a$.

The situation when $2 < m_d < 3$, namely, $m_d = 2.5$ is shown in Fig. 9c. One branch of the amplifier $1g$ and one of the three branches of the absorber $1a$, $2a$ or $3a$ will be involved in this case. The cycle formed on the branch $3a$ yields a reduction of the pulse duration. This happens because the pulse moving from amplifier to absorber has the area $\Phi > 2\pi$. During its propagation in the absorber Φ will tend to 2π and the pulse duration will decrease. Thus, the ratio of the dipole moments influences the duration of the laser pulse in a coherent mode-locking.

In the situation when $m_d > 3$ (not shown) the branch $4a$ can participate in generation. On this branch, the formation of radiation with area 4π takes place, which must split into two 2π pulses

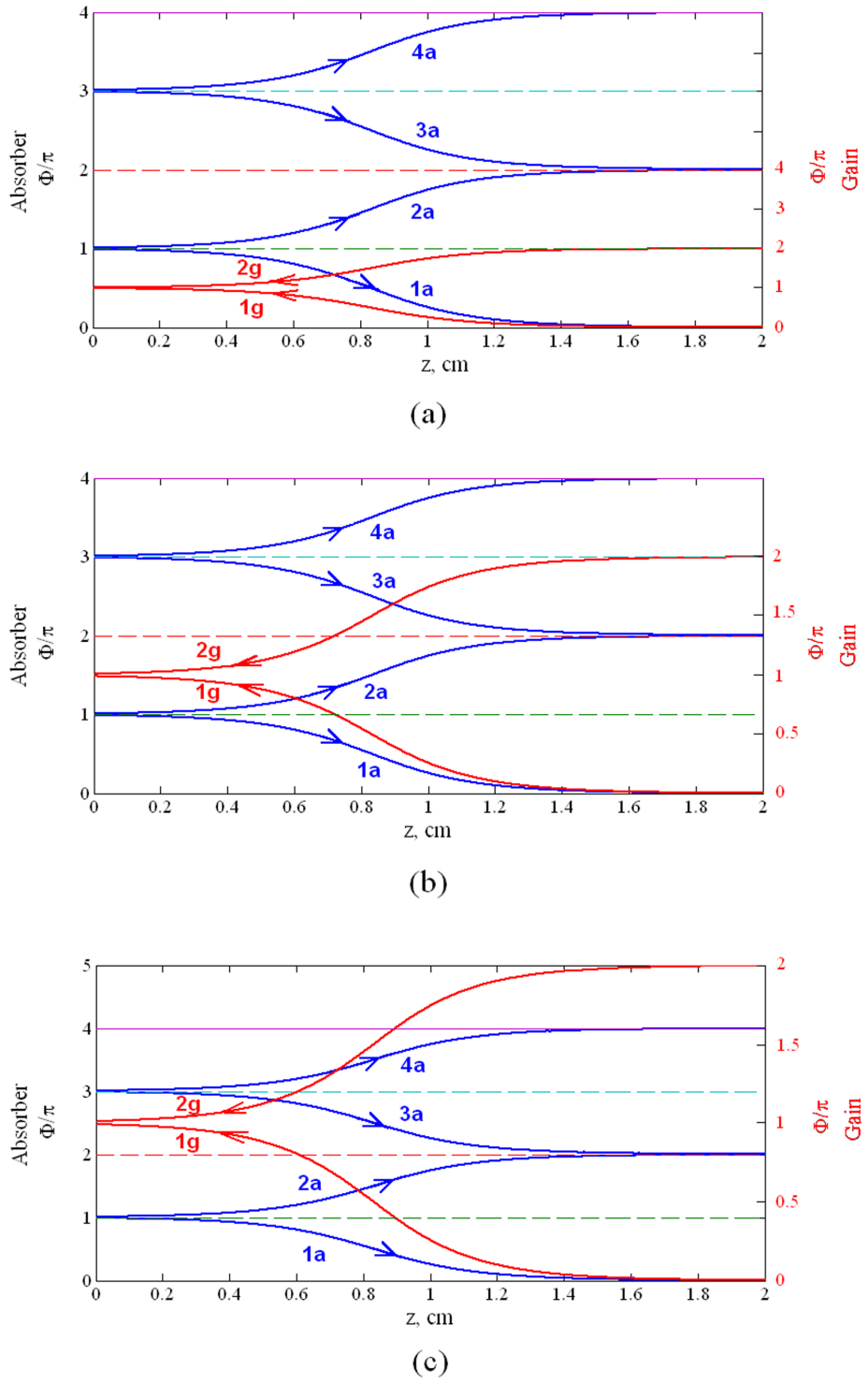

Figure 9: Branches of solution of Eq. (2) for an absorber (blue lines) and amplifying medium for different ratios m_d. (a): $m_d = 0.5$, (b): $m_d = 1.5$, (c): $m_d = 2.5$.

which might have different amplitudes and durations. Thus, in this situation two pulses will arise over a single cavity round-trip.

It is to be remarked that the McHall and Hahn diagrams demonstrated above were first introduced in the present work and provide a unifying framework allowing better understanding of the passive mode-locking process in the coherent regime. It demonstrates the stability of the pulsating regimes over the wide range of parameters. Sometimes such stable pulsations are obtained even without an external seed.

3 Fundamental equations for laser model

To study the mechanism of mode-locking in a two-section laser we carry out numerical experiments based on a set of Maxwell-Bloch equations describing propagation of light in a two-level medium in a slow-varying envelope approximation for the field and for the atomic polarization [15–17, 44, 46, 62–65].

The set of equations governing its evolution has the form:

$$\frac{d}{dt}P_c^{\pm}(z,t) = -\frac{P_c^{\pm}(z,t)}{T_2} - \Delta\omega P_s^{\pm}(z,t) - \frac{d_{12}}{2\hbar}\Delta\rho(z,t)B^{\pm}(z,t), \tag{8}$$

$$\frac{d}{dt}P_s^{\pm}(z,t) = -\frac{P_s^{\pm}(z,t)}{T_2} + \Delta\omega P_c^{\pm}(z,t) + \frac{d_{12}}{2\hbar}\Delta\rho(z,t)A^{\pm}(z,t), \tag{9}$$

$$\begin{aligned}\frac{d}{dt}\Delta\rho(z,t) = -\frac{\Delta\rho(z,t)-\Delta\rho_0}{T_1} - \frac{2d_{12}}{\hbar}(A^+(z,t)P_s^+(z,t) + A^-(z,t)P_s^-(z,t) + \\ +B^+(z,t)P_c^+(z,t) + B^-(z,t)P_c^-(z,t)),\end{aligned} \tag{10}$$

$$\frac{\partial A^{\pm}(z,t)}{\partial t} \pm c\frac{\partial A^{\pm}(z,t)}{\partial z} = -4\pi\omega d_{12}N_0 P_s^{\pm}(z,t), \tag{11}$$

$$\frac{\partial B^{\pm}(z,t)}{\partial t} \pm c\frac{\partial B^{\pm}(z,t)}{\partial z} = 4\pi\omega d_{12}N_0 P_c^{\pm}(z,t). \tag{12}$$

Equations (8)-(10) describe the evolution of slowly varying envelopes of two counter-propagating waves (in-phase $P_c^{\pm}(z,t)$ and quadrature $P_s^{\pm}(z,t)$ components) of real and imaginary parts of non-diagonal element of the quantum mechanical density matrix, as well as the population difference $\Delta\rho$ between the lower and upper energy levels of the medium. Equations (11) and (12) govern the evolution of amplitudes (in-phase $A^{\pm}(z,t)$ and quadrature $B^{\pm}(z,t)$ components) of the two counter-propagating optical waves. The propagation direction is denoted by $(+)$ and $(-)$ respectively. The derivation of the model equations is given in Appendix A. The equations include parameters of the two-level system, such as transition dipole moment d_{12}, concentration of two-level atoms N_0, population difference relaxation time T_1, polarization relaxation time T_2, carrier frequency of the optical field ω, frequency detuning $\Delta\omega$ of the radiation field from transition frequency of the two-level medium ω_{12}, and population difference at the equilibrium $\Delta\rho_0$. For the amplifying medium, $\Delta\rho_0 = -1$, for the absorbing medium, $\Delta\rho_0 = 1$. We make

all these parameters depending on the space coordinate z, so that these equations can be applied to the description of the gain and the absorbing medium located in different sections of the cavity. The set of equations (8)-(12) affords sufficiently complete modeling of evolution of extended two-level media in a cavity, taking into account multi-mode character of radiation and the nonlinear coherent effects accompanying interaction of the light with the two-level medium. It was also used in our recent study of lasing without population inversion in a two-level optically dense medium [66], and spectral condensation phenomenon arising when narrow-band absorbing medium is placed in the resonator with broad-band amplifying medium [67].

We apply the system of equations (8)-(12) to analyze the situation when both laser gain and absorber media are placed in the ring optical cavity in the case of unidirectional propagation, as well as the case of a linear cavity. In our analysis below we will assume that resonance frequencies in the gain and absorber are equal to each other and to the carrier frequency of the electric field, i.e. $\Delta\omega = 0$. The simplified system of Maxwell-Bloch equations under these conditions can be written in the form:

$$\frac{\partial A^{\pm}(z,t)}{\partial t} \pm \frac{\partial A^{\pm}(z,t)}{\partial z} = 4\pi\omega_{12} d_{12} N_0 P_s^{\pm}(z,t), \tag{13}$$

$$\frac{d}{dt} P_s^{\pm}(z,t) = -\frac{P_s^{\pm}(z,t)}{T_2} + \frac{d_{12}}{2\hbar}\Delta\rho(z,t) A^{\pm}(z,t), \tag{14}$$

$$\frac{d}{dt}\Delta\rho(z,t) = -\frac{\Delta\rho(z,t) - \Delta\rho_0}{T_1} - \frac{2d_{12}}{\hbar}\left(A^{+}(z,t)P_s^{+}(z,t) + A^{-}(z,t)P_s^{-}(z,t)\right). \tag{15}$$

4 Coherent mode-locking in lasers with a ring cavity

In the case of a ring cavity we put in Eqs. (8)-(12) $A^{-}(z,t) = 0$, assuming thus unidirectional propagation and using the notation $A^{+}(z,t) \equiv A(z,t)$. First, we consider the case when the ratio of the transition dipole moments absorber/gain $m_d = 2$. We perform numerical simulations of the model equations (8)-(12) for the parameter values given in Table 1 and Table 2.

Table 1: Parameter values used in the numerical simulations

Parameter	Gain	Absorber
central wave length of the medium	$\lambda_{12g} = 0.7\ \mu m$	$\lambda_{12a} = 0.7\ \mu m$
length of the medium	$L_g = 0.15$ cm	$L_a = 0.45$ cm
concentration of two-level atoms	$N_{0g} = 12.5 \cdot 10^{14}$ cm^{-3}	$N_{0a} = 12.5 \cdot 10^{14}$ cm^{-3}
transition dipole moment	d_{12g} = 5 Debye	d_{12a} = 10 Debye
population difference at equilibrium	$\Delta\rho_{0a} = 1$	$\Delta\rho_{0g} = -1$
population difference relaxation time	$T_{1g} = 0.16$ ns	$T_{1a} = 0.16$ ns
polarization relaxation time	$T_{2g} = 40$ ps	$T_{2g} = 40$ ps

Assuming also the initial conditions with the constant amplitude close to non-lasing solution, we perform numerical simulations showing that after a transition process taking a few tens of cavity round-trip times, regular sequence of short optical pulses appears. The pulse-to-pulse period of this pulse train is larger than the cold cavity round-trip time $T = L/c = 20$ ps. Since we

Table 2: To Table 1

cavity length L = 0.6 cm
reflectivity of the mirror R = 0.8
initial pulse area $\Phi_0 = 10^{-10}\pi$

assumed $T_{2g} = T_{2a} = 40$ ps, which is larger than T and also an order of magnitude more than the pulse duration (1 ps), the interaction of light and matter is in coherent regime and accompanied by the formation of pulses with the area close to 2π in the absorber and π in the amplifier.

Fig. 10a,b illustrates the spatial distribution of $A(z)$, $\Delta\rho(z)$ and $P_s(z)$. In Fig. 10a the laser pulse passes through the absorber whereas in Fig. 10b it is located in the amplifier (the pulse moves from left to right during the propagation). Fig. 10 shows the pulse at the time moment close to the 100th round-trip after the beginning of the numerical simulations, when the stable pulsing regime is already established. At the leading edge of the pulse the population difference $\Delta\rho$ decreases until the value close to -0.8. $P_s > 0$ in this interval, hence, absorption of the radiation takes place. At the trailing edge $P_s < 0$, and the population difference increases and is recovered to its initial value. The absorber starts to radiate, returning energy to the trailing edge of the pulse. Thus the pulse shown in Fig. 10 has all the features of the SIT one.

After passing through the absorber the pulse propagates in the amplifier, see Fig. 10b. It can be seen that at the trailing edge of the pulse the population inversion $\Delta\rho$ becomes positive. P_s is, on the other hand, negative, therefore, the medium gives the energy to the field. The gain medium becomes absorbing after the pulse passage. This behavior is typical for the π pulse propagating in the amplifying medium.

Fig. 10c illustrates the dependence of the pulse area inside the cavity during a single pass. It is clearly seen that, as it was predicted in the previous section, the pulse area is close to 2π in the absorber and to π in the gain. A pulse with the area noticeably smaller than 2π arrives to the entrance of the absorber and then its area rapidly grows. Interestingly, the pulse area in the amplifier increases somewhat but then start to decrease. The initial increase above the value of π is because of the finite relaxation time of the media. The subsequent decrease is due to self-stabilization mechanism of the π-pulse area.

Fig. 10d shows the distribution of the electric field amplitude $A(z)$ in the cavity over four round-trips. It demonstrates one more feature of the pulse propagation inside the cavity, namely that the pulse velocity in the absorber is smaller than in the amplifier, which manifests itself in a bend of the pulse propagation trajectory on the boundary between the absorber and amplifier.

Another important feature should be mentioned in this case. The spectrum of the laser generation is much broader than the width of the gain (absorption) profile since pulse duration $\tau_p \sim 1$ ps is smaller than medium coherence time $T_{2g} = T_{2a} = 40$ ps in this case. This can be seen from Fig. 11a,b, where the time dependence of the output field intensity $|A|^2$ and its spectrum together with the Lorentzian gain and absorption line shapes are plotted. In the usual passive mode-locking theory the situation is different — the pulse duration is determined by the bandwidth of the gain medium. Also, it is seen from Fig. 11b that the pulse repetition frequency is smaller than cold-cavity one (50 GHz) because of the fact that pulse in the absorber propagates

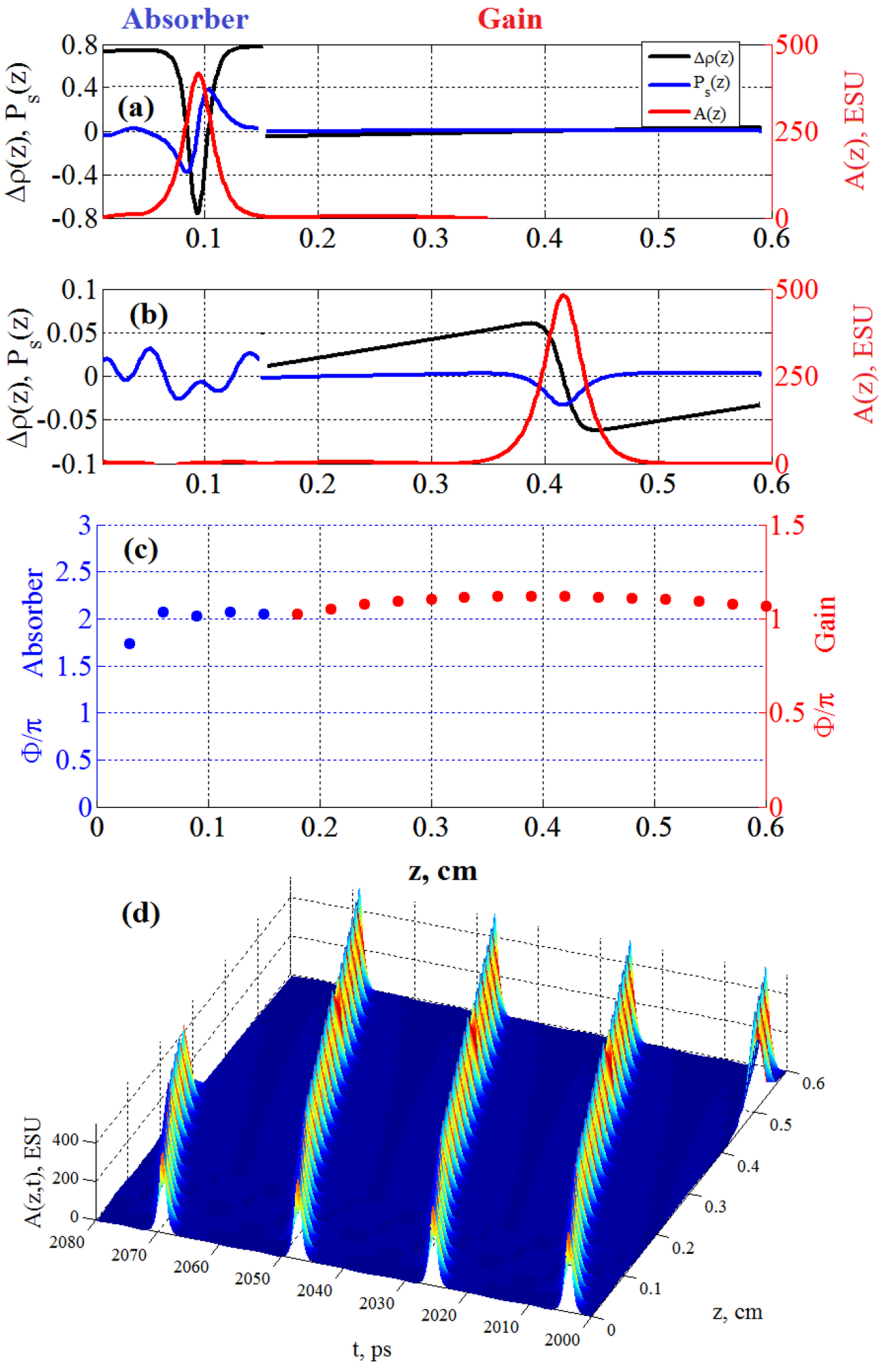

Figure 10: (a), (b) Distribution of the electric field amplitude $A(z)$ in the cavity (red line), $P_s(z)$ (blue line) and population difference $\Delta\rho(z)$ (black line) when pulse is located in the absorber (a) and in the gain (b) sections. (c) Evolution of the pulse area in the cavity during one round-trip. (d) Distribution of the electric field amplitude $A(z)$ field in the cavity. The parameter values given in Table 1 and in Table 2.

with the velocity smaller than c. In the amplifier π-pulse propagates with the velocity of light c.

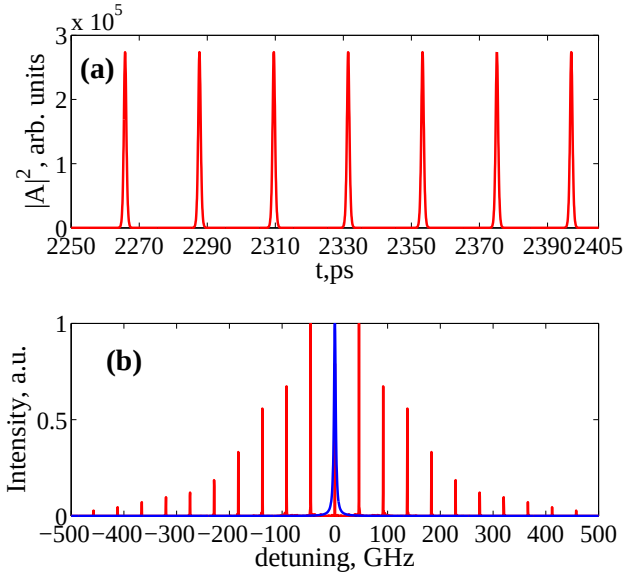

Figure 11: (a) Time dependence of the output field intensity. (b) Its spectrum (red) and normalized Lorentzian gain and absorption line shapes (blue) for the example illustrated in Fig. 10.

Fig. 10b shows that the value of polarization in the absorber after the pulse passage is not equal to zero due to the fact that some of the pulse energy is left in the absorber [43]. It changes its sign along the medium and has relatively large value resulting in an additional light emission by the absorber. This is so-called "coherent optical ringingöf the field and polarization [68]. Coherent ringing creates radiation that propagates in the direction of the amplifier. However, immediately after the passage of the pulse the amplifier is still absorbing, resulting in attenuation of this radiation. Besides, the radiation remaining in the absorber will affect the propagation of the pulse when it appears in the absorber again. This fact can be seen from our simulations on the behavior of the pulse area in the absorber (see Fig. 10c), which is non-monotonic. One can see an increase of such “jitter” with the increase of the absorber length. On the other hand, the effect of coherent ringing decreases with decrease of T_2. Note that such “noise of polarization” created by a laser pulse in the absorber is characteristic for the coherent mode-locking. And its influence on the coherent mode-locking regime we report for the first time. Numerical simulations for the case of mixed gain and absorber in the soliton laser shows a large value of such ringing. A detailed quantitative analysis of the impact of coherent ringing on the pulse dynamics is a subject of a separate study and is not considered in this paper.

The example presented above demonstrates the existence of coherent mode-locking in a ring optical laser geometry with unidirectional lasing and the gain spatially separated from absorber, in contrast to previous works. One of the most important parameters influencing the dynamics is the time relaxation of polarization in the gain and absorber. In the example shown in Fig. 10 $T_{2a} = T_{2g} = 40$ ps. Our numerical simulations show that the regime of short optical pulses is preserved if these times are independently varied from 2 ps until 50 ps. Influence of the relaxation time $T_2 = T_{2g} = T_{2a}$ on the pulse parameters in the coherent mode-locking regime

is shown in Fig. 12, where the half-width pulse maximum duration τ_p, its peak intensity I_p, and energy density W is shown in the steady state regime after 100 round-trips times.

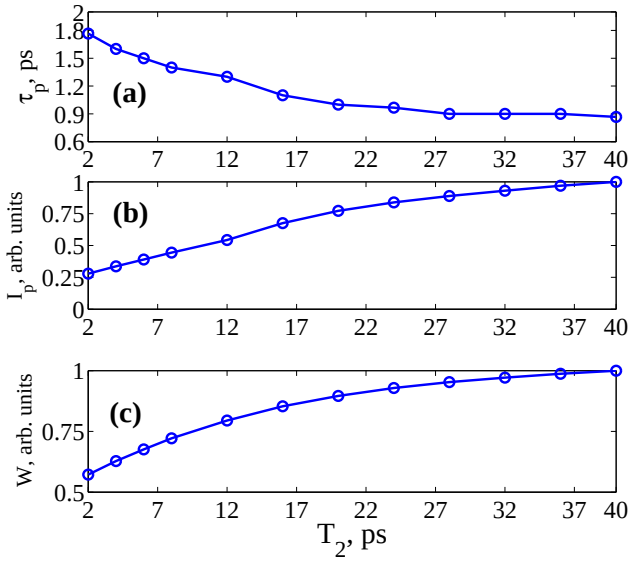

Figure 12: Dependence of the pulse duration τ_p (a), the peak intensity I_p (b) and energy density of the pulse W (c) on the polarization relaxation time $T_2 = T_{2g} = T_{2a}$. Other parameter values are as in Table 1 and Table 2.

It is seen from Fig. 12 that the pulse duration increases with the decrease of T_2, whereas the peak intensity and the energy density decreases. This behavior can be explained by the fact that with decrease of the "phase memory time" T_2 the part of the energy transferred to the absorber at the leading edge and coming back at the trailing edge decreases, which in turn influences the gain. The behavior of the pulse area in the cavity under different values of T_2 is further illustrated in Fig. 13. One can see that this dynamics is quite similar for very different values of T_2.

Fig. 14 presents the dependence of the pulse duration τ_p (a), peak intensity I_p (b) and pulse energy density W (c) on the ratio of the dipole moments of the absorber and amplifier m_d. We see that with increasing of d_{12a} the pulse duration decreases from 1.35 ps to 200 fs. This leads to the increase of the peak intensity approximately 4 times, thus keeping the pulse energy approximately constant, see Fig. 14c. Numerical simulations were performed using the parameter values $T_{2g} = 20$ ps, $N_{0g} = N_{0a} = 18 \cdot 10^{14}$ cm^{-3}. Other parameter values are as in Table 1 and in Table 2.

Let us consider the case when the ratio of the dipole moments of the absorber/gain $m_d < 1$. In this case, according to the area theorem, the pulse area in the absorber must tend to zero. The example of the numerical simulations of the model equations (8)-(12) when $d_{12a} = 2.5$ Debye ($m_d = 0.5 < 1$) with other parameters are as in Table 1 is given in Fig. 15. Fig. 15a illustrates the distribution of the pulse amplitude in the different parts of the cavity. In particular, in the absorber, according to the area theorem, the pulse area tends to zero and increases to π in the gain section, see Fig. 15b. Our numerical simulations indicate that there are two pulses with different values of the peak intensity for one round-trip time at the output from the gain medium,

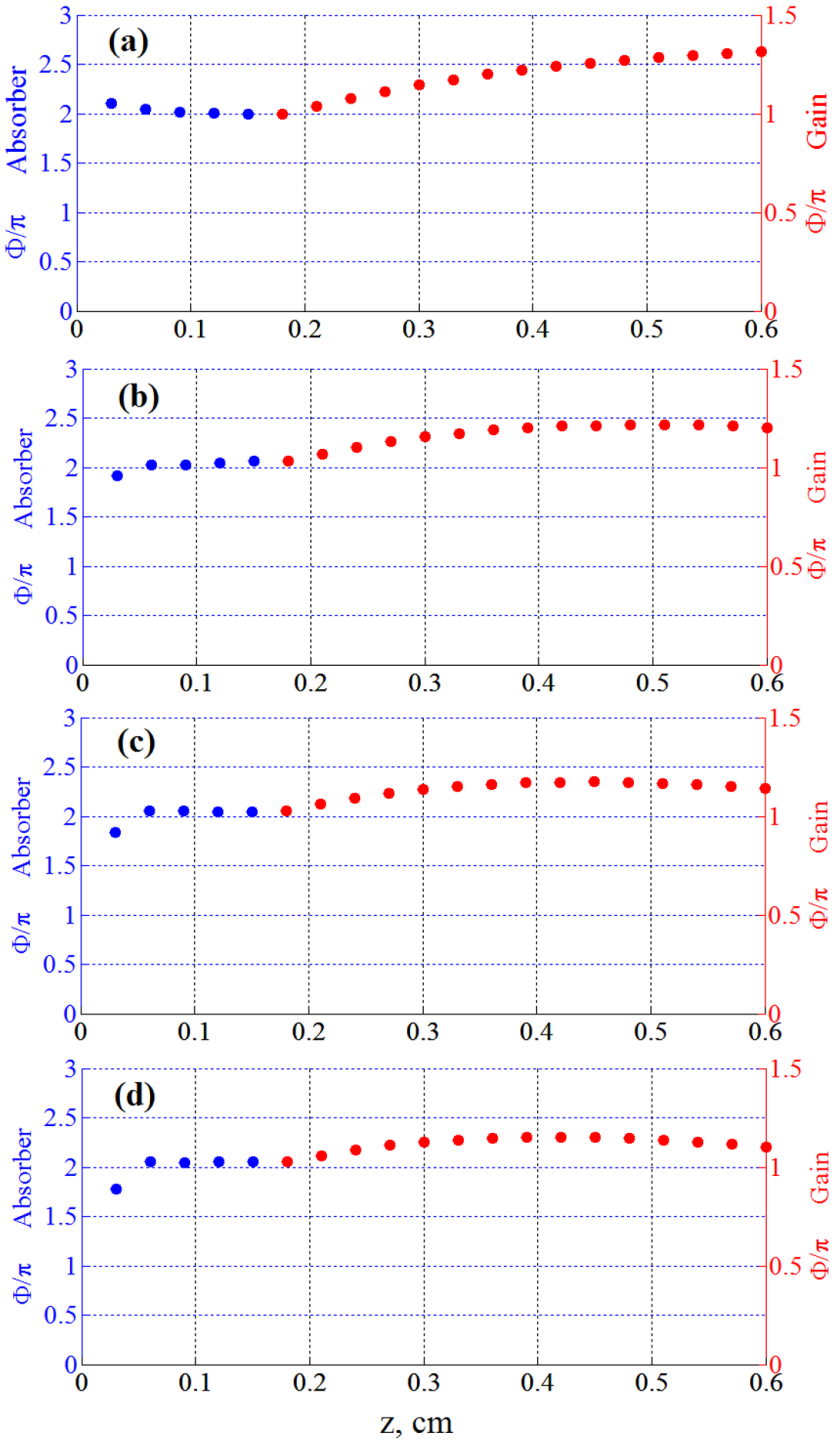

Figure 13: Dependence of the pulse area in the cavity Φ under different values of $T_2 = T_{2g} = T_{2a}$. (a): $T_2 = 4$ ps, (b): $T_2 = 8$ ps, (c): $T_2 = 12$ ps, (d): $T_2 = 16$ ps. Other parameter values are as in Table 1 and Table 2.

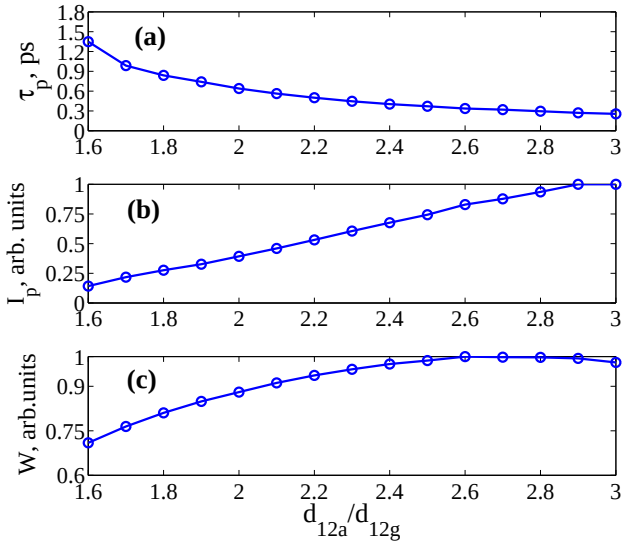

Figure 14: Dependence of the pulse duration τ_p (a), the peak intensity of the pulse I_p (b) and energy density of the pulse W (c) on the ratio of the dipole moment of the absorber and gain medium m_d. $T_{2g} = 20$ ps, $N_{0g} = N_{0a} = 18 \cdot 10^{14}$ cm^{-3}. Other parameter values are as in Table 1 and Table 2.

see Fig. 15c.

Finally, let us consider the case when the ratio of dipole moments $m_d > 3$, namely $m_d = 4$. In this situation McCall and Hahn diagrams predict appearance of two pulses. Fig. 16 illustrates the results of numerical simulations when $d_{12a} = 20$ Debye with other parameters are as in Table 1. Generation has the form of a periodic train of pulse pairs, one for each cavity round-trip time, see Fig. 16c. The pulse area in the absorber is close to 4π and tends to π in the gain section as shown in Fig. 16c.

In conclusion, numerical experiments using the system of Maxwell-Bloch equations in the slowly varying envelope approximation shows the presence of a stable coherent mode-locking in a two-section ring-cavity laser with absorbing and amplifying media separated in space. Mixing of these media, as it was done in the pioneer works in Refs. [53, 54] is not necessary for the coherent mode-locking to arise. Moreover, in such two-section laser injection of a seed pulse is also not a necessary condition for the appearance of pulsed regime. In contrast, self-starting from noise is possible. Remarkably, the width of the lasing spectrum can be significantly broader than the width of the gain line. Coherent mode-locking regime is preserved even if the relaxation time of the polarization in the amplifier and absorber either larger or smaller than the round-trip time of the cavity. In examples presented above T_2 of the media varied from 40 ps to 2 ps at a cavity round-trip time 20 ps.

We also have demonstrated the influence of the dipole moments absorber/gain ratio m_d on the coherent mode-locking regime. In the range $1.5 < m_d < 3$ an increase of m_d leads to a decrease of the laser pulse duration. Our numerical simulations indicate that the coherent mode-locking regime is also possible if $m_d < 1.5$ and $m_d > 3$. However, in this case several

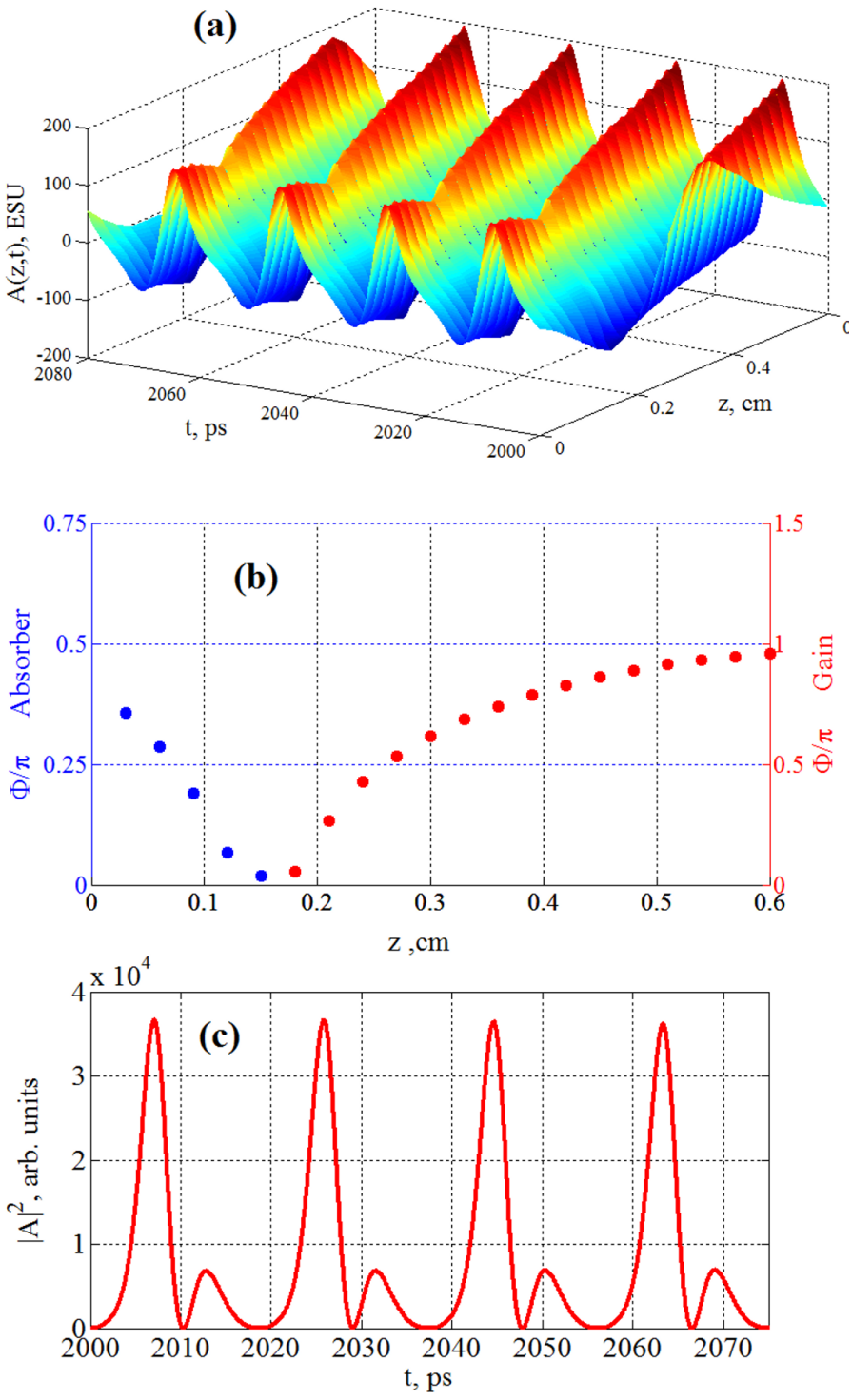

Figure 15: Evolution of the electric field amplitude in the cavity $A(z,t)$ (a), Dependence of the pulse area $\Phi(z)$ inside the cavity (b) and the temporal dependence of the output intensity $|A|^2$ (c) for $d_{12a} = 2.5$ Debye and other parameter values given in Table 1 and Table 2.

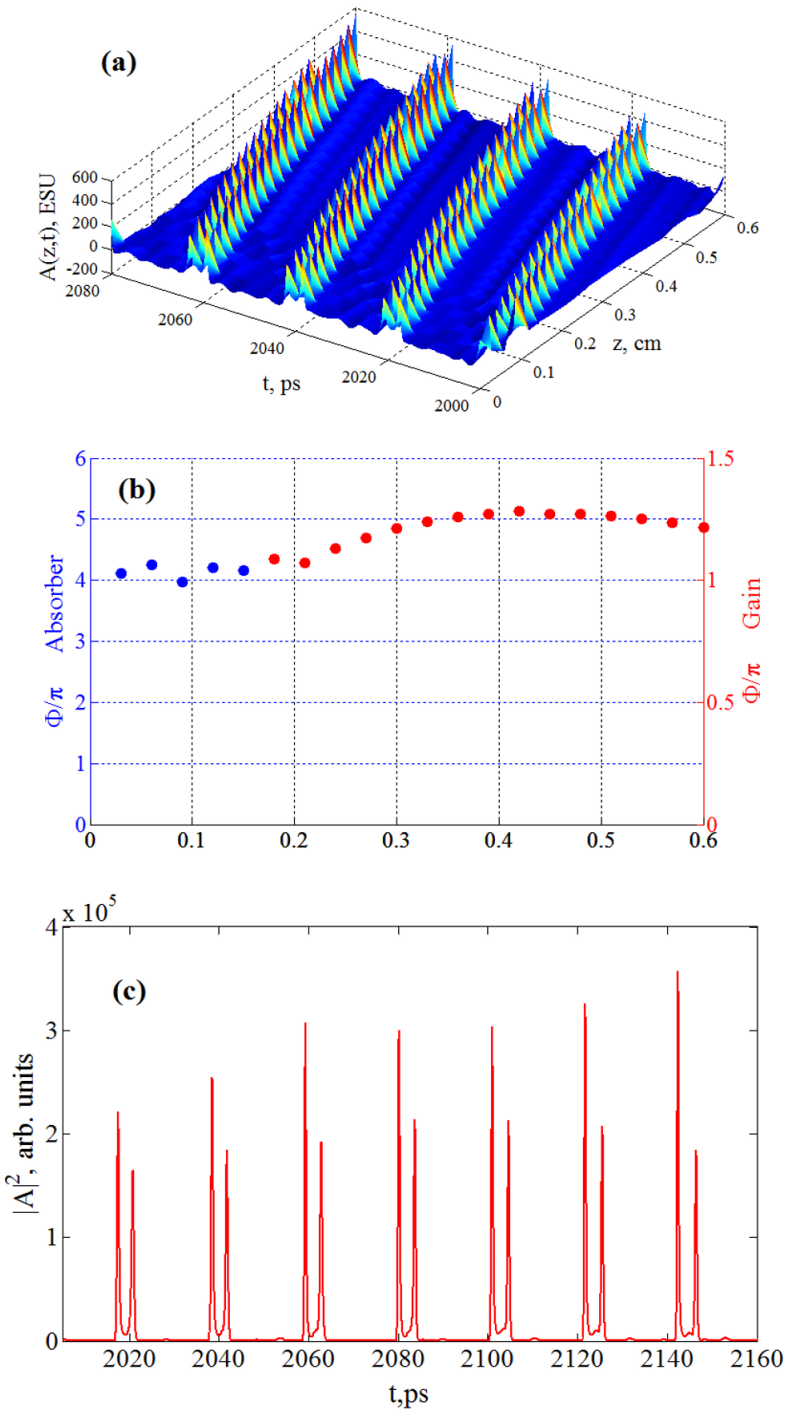

Figure 16: Evolution of the electric field amplitude in the cavity $A(z,t)$ (a), Dependence of the pulse area $\Phi(z)$ inside the cavity (b) and the temporal dependence of the output intensity $|A|^2$ (c) for $d_{12a} = 20$ Debye and other parameters given in Table 1 and Table 2.

pulses per cavity round-trip time occur.

5 Modeling coherent mode-locking in a laser with a linear cavity

In the previous sections we considered a two-section laser with a circular geometry. Here we consider an another scheme namely a linear laser geometry. To perform numerical simulations, we use the system (13)-(15) with both propagation directions retained.

There is an important difference between a laser with a linear cavity and a ring one. In case of a ring cavity (Fig. 17a) a pulse coming out of the gain medium passes first the absorber section and only then reenters the gain. In such a way, some time is gained for the relaxation processes in the gain section. During this time the gain in the medium recovers under the action of pumping, and the medium becomes an amplifier again.

Another situation arises in the linear cavity, see Fig. 17b. Consider what happens in the amplifying medium when it almost completely fills the cavity. Assume that a pulse propagates in the amplifying medium from the point A to B. This pulse, leaving the point B, is reflected from the mirror and goes back to the point B again. At this time the gain medium near B has not recovered yet, and thus no amplification arises. As a result, intensity of the pulse does not increase near the point B. In contrast, near A the gain has already recovered, so that finally net amplification may still take place in the amplifier. Amplification around point B will also takes place for the pulse, when it comes from the opposite direction. As a consequence, the existence of two counter-propagating pulses is possible in this situation, which is shown in this section by the means of numerical simulations.

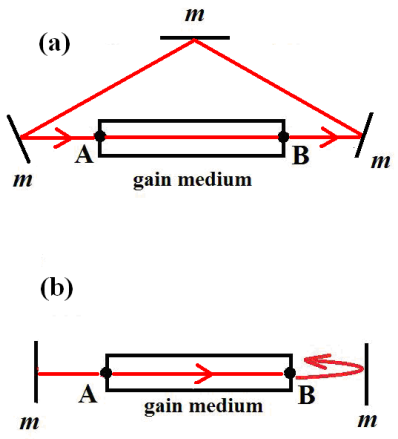

Figure 17: Schematic representation of pulse motion in a ring (a) and linear lasers (b). by m the cavity mirrors are marked.

In the numerical simulations we consider a situation when the amplifier section is placed in the center of the cavity (as Fig. 18a but without absorber), and the cavity mirrors have the same

reflection coefficients. Numerical experiment visualized in Fig. 18a demonstrates a stable self-mode-locking regime with the pulse-to-pulse distance equal to the half of the cavity round-trip time. The pulse repetition rate is explained by the appearance of pulses in both of the counter-propagating waves.

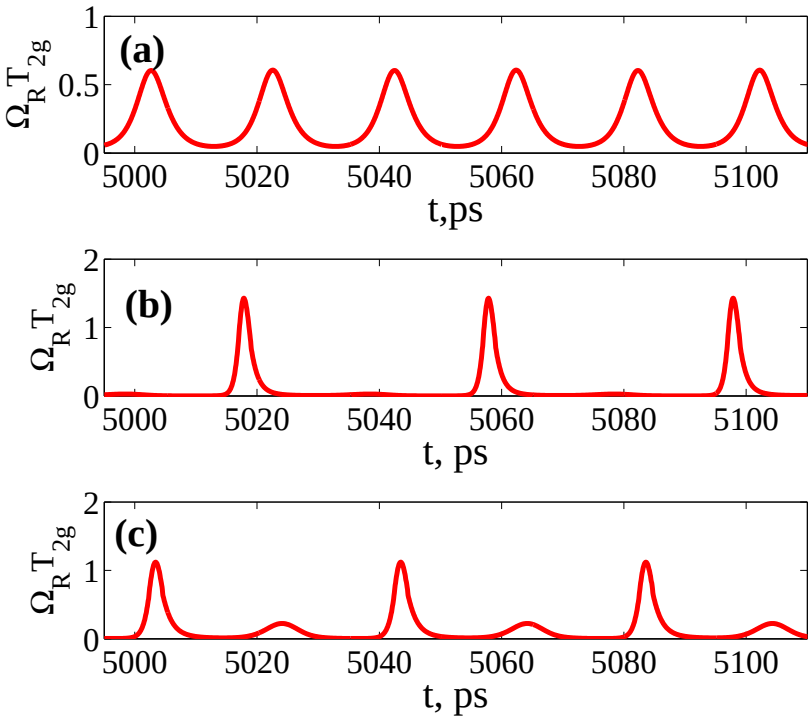

Figure 18: Results of the numerical simulations of the laser generation with a linear cavity. On the y-axis is the value of the Rabi frequency $\Omega_R = d_{12g}A/\hbar$ normalized to T_{2g}. Parameters of the model: cavity length $L = 0.6$ cm, length of the gain medium $L_g = 0.15$ cm, optical wavelength $\lambda = 0.7\mu$m, reflectivity of the laser mirrors: $R = 0.6$, $T_{1g} = 0.5$ ns, $T_{2g} = 1$ ps, $d_{12g} = 5$ Debye, $N_{0g} = 15 \cdot 10^{15}$ cm^{-3}. (a) The stable pulsation regime in the case when only the gain section is present in the cavity. The period of the pulse train is 20 ps and equal to the half of the round-trip time. (b) Active mode-locking due to modulation of the reflectivity of one of the cavity mirrors with 20 percent depth and the period equal to the cavity round-trip time $(40$ ps). The repetition rate of the pulse train is now equal to the one of external modulations. (c) Passive mode-locking in a two-section laser shown in Fig. 18a. The length of the absorber is L_a=0.15 cm, and $T_{1a} = 0.6$ ns, $T_{2a} = 0.5$ ps, $d_{12a} = 5$ Debye, $N_{0a} = 5 \cdot 10^{15}$ cm^{-3}.

In order to suppress one of the pulses we may, for instance, introduce an external modulation of the reflectivity of one of the mirrors with the period close to the cold-cavity repetition period $2L/c$. In this way we introduce elements of active mode-locking. In this case due to competition between the pulses in the cavity there remains only one pulse, for which the mirror reflectivity is maximal at the moment of the pulse incidence, see Fig. 18b. The counter-propagating wave can also be suppressed if an absorbing section is placed between one of the mirrors and the

amplifier, as shown in Fig. 18c.

The solutions presented in Fig. 18 shows that the absorber creates a regime in which only one pulse propagates in the cavity. The peak amplitude value of this single pulse is larger and pulse duration is smaller than in the case of two pulses.

One should note that in the situation considered above the laser operates in incoherent regime, since the laser pulse duration is larger than the medium coherence time T_2. In particular, the population difference does not change its sign (because $\Omega_R \cdot T_{2g} \simeq 1$ in Fig. 18). The electric field amplitude A, slow envelope of the imaginary part of the non-diagonal element of density matrix P_s as well as population difference $\Delta\rho$ for the case given in Fig. 18c are shown in Fig. 19 for various positions and directions of the pulse propagation inside the cavity.

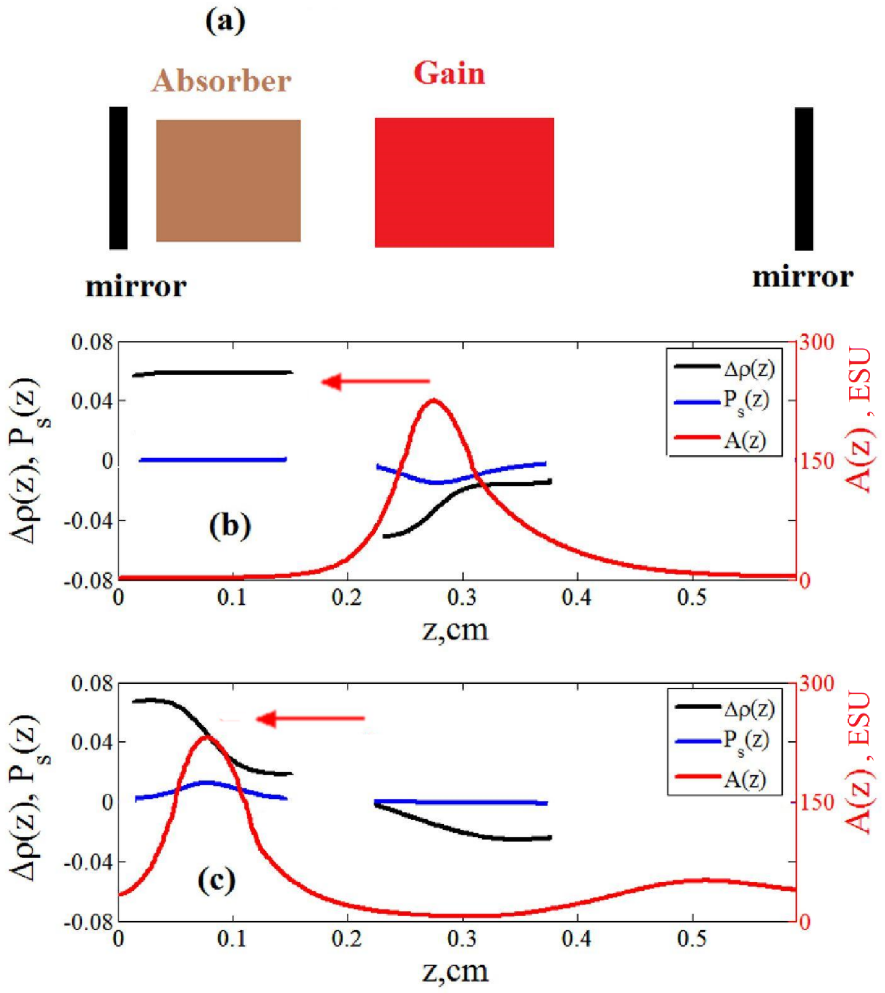

Figure 19: Distribution $A(z) = A^+(z) + A^-(z)$, $P_s(z) = P_s^+(z) + P_s^-(z)$ and $\Delta\rho(z)$ in the laser with the linear cavity in the regime of steady-state generation during a single pass. All the parameters are the same as in Fig. 18. (a) The scheme of the laser. The pulse is shown as it propagates from right to left and is located in the gain medium (b) and, at the later time moment, when it is located in the absorbing medium (c). Red arrow indicates the direction of pulse propagation.

One can expect the appearance of coherent mode-locking if we increase significantly the amplitude of the pulse. For this, we may increase the concentration of the particles in the amplifier and absorber (and set them equal to each other) and make the dipole moment of the absorber twice larger than that of the amplifier. The later is very important for the realization of coherent mode-locking as shown in the previous section. The results of numerical simulations in such modified system are shown in Fig. 20. By changing the model parameters in this way mode-locking is in the regime of coherent interaction of light and matter, both in the amplifier and in the absorber.

Another example of the coherent mode-locking regime is given in Fig. 21. In contrast to the previous case the polarization relaxation time in the absorber T_{2a} and the concentration of absorbing particles N_{0a} were increased. Such parameter modifications do not lead to disappearance of passive mode-locking, but modify the scenario of the pulse propagation in the cavity in the mode-locking regime and the pulse shape at the output of the laser. During the evolution the pulse exits the amplifier and enters the absorber with the area close to 2π (for the absorber), see Fig. 21a. Due to the losses at the left mirror ($R = 0.6$) during the back trip the pulse propagates in the absorber as a π-pulse. The leading edge of the pulse loses energy and inverts the medium. Behind the pulse, coherent polarization begins to emit electromagnetic radiation which is in anti-phase to the pulse, see Fig. 21b. As a result, at the input of the amplifier the pulse has the area close to zero, see Fig. 21c. Propagation of this pulse in the amplifying medium has the following features: the part of the pulse envelope with a negative sign is amplified not so efficiently as the leading edge, Fig. 21d. In the amplifier the pulse area increases and tends to π. As a result, at the laser output a train of intense short pulses with a small burst at the trailing edge is observed. After the reflection from the mirror the pulse area decreases, but during the pulse propagation in the amplifier it tends to a π pulse again, see Fig. 21e-Fig. 21f.

The burst at the trailing edge of the pulse disappears if the reflectivity on the left facet of the laser is 1. The scenario of the pulse propagation changes in the following way: from the amplifier to the absorber comes a pulse, which behaves in the absorber like 2π pulse, see Fig. 22a. After the reflection from the left-side mirror the pulse does not change its area and propagates as a 2π-like pulse in the absorber, Fig. 22b. Due to the finite relaxation time of the absorber the pulse area changes only slightly during the propagation in the absorber, and the sign change of the field envelope does not occur, see Fig. 22b. Then the pulse propagates in the gain section as a π pulse, see Fig. 22c-Fig. 22d. After the reflection from the mirror and propagation through the amplifying medium (Fig. 22e) a π pulse is formed (Fig. 22f). This pulse propagates as a 2π pulse in the absorber and the propagation cycle is repeated again.

In these examples the relaxation time of polarization was very close to the pulse duration (~ 1 ps). In this situation the coherent mechanism of the light-matter interaction plays a major role. However, the scenario of pulse formation differs from the case of a ring laser, considered in the previous section. The particular difference is that the existence of π (2π) pulses along the whole length of the amplifier (absorber) is not required for a passive mode-locking to arise.

Importantly, the examples of the coherent mode-locking presented in this section were reproduced by us in the large parameter range, in particular for the parameter values typical for semiconductor, solid states and gas lasers.

Besides, our numerical experiments show that the regime of coherent mode-locking is preserved

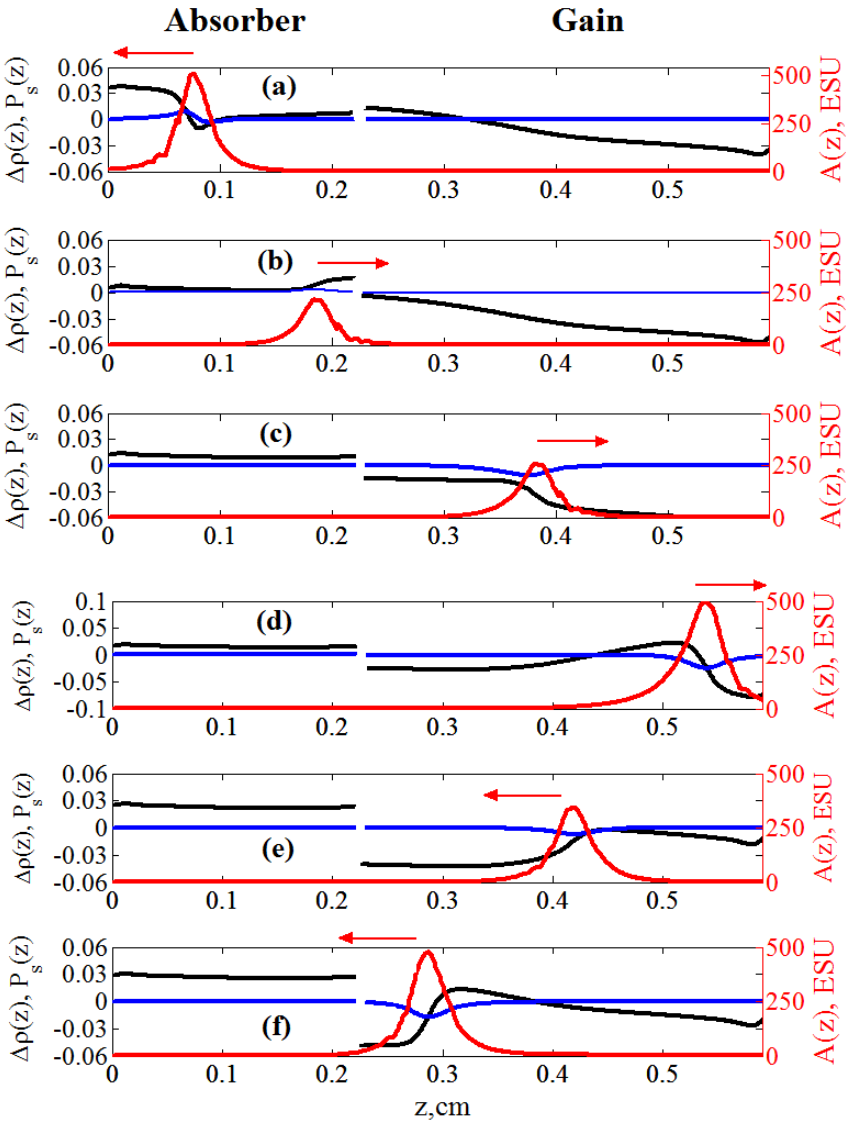

Figure 20: Distribution of the electric field amplitude $A(z) = A^+(z)+A^-(z)$ (red line), $P_s(z) = P_s^+(z)+P_s^-(z)$ (blue line) and $\Delta\rho(z)$ in the laser with the linear cavity in the regime of steady-state generation during one pass ($\lambda = 0.7\mu m$, $R = 0.6$, $T_{1g} = 0.5$ ns, $T_{2g} = 1$ ps, $d_{12g} = 5$ Debye, $L_g = 0.36$ cm, $T_{1a} = 1$ ns, $T_{2a} = 0.4$ ps, $d_{12a} = 10$ Debye, $L_a = 0.22$ cm, $N_{0g} = N_{0a} = 15 \cdot 10^{15}$ cm^{-3}). In (a) - (f) the consequent stages of the pulse propagation are shown, with different propagation direction (which is alternated by reflections) and pulse position in the absorber and amplifier. Red arrow indicates the direction of pulse propagation.

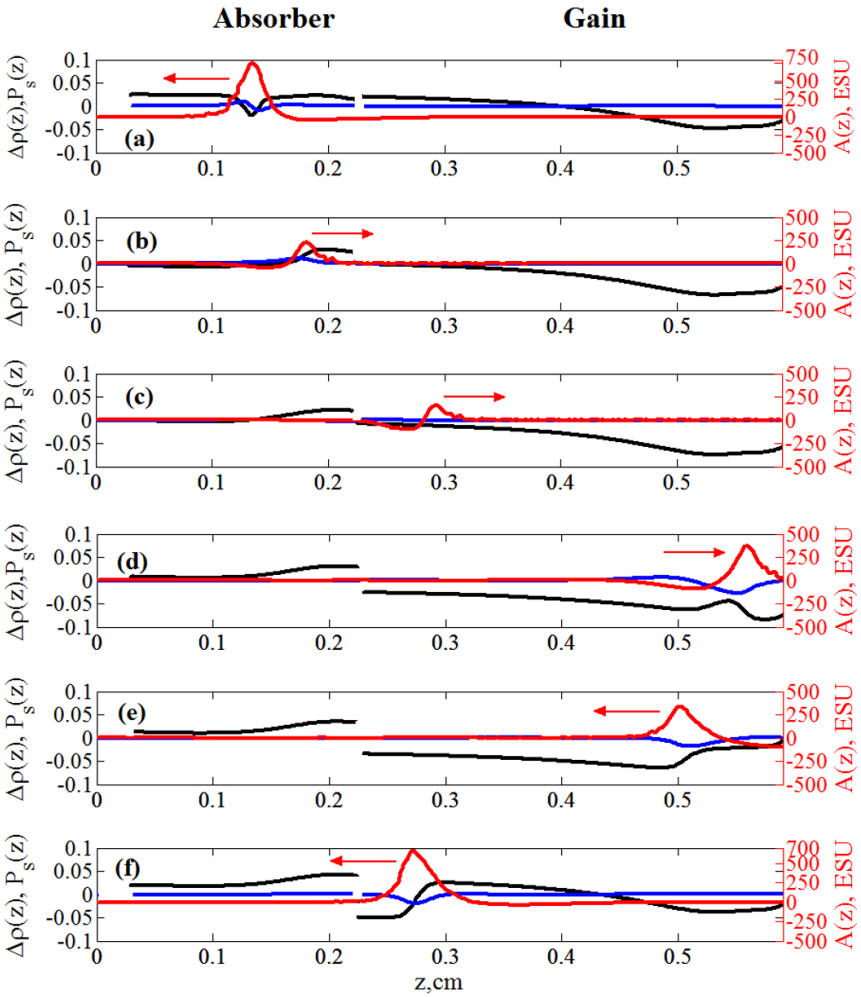

Figure 21: (a)-(f) Distribution of the electric field amplitude $A(z)$ (red line), polarization amplitude $P_s(z)$ (blue line) and population difference $\Delta\rho(z)$ in the laser with a linear cavity in the coherent mode-locking regime during a single round-trip for different pulse positions and propagation directions for $\lambda = 0.7\mu m$, $R = 0.6$, $T_{1g} = 0.5$ ns, $T_{2g} = 1$ ps, $d_{12g} = 5$ Debye, $L_g = 0.36$ cm, $N_{0g} = 15 \cdot 10^{15}$ cm^{-3}, $T_{1a} = 1$ ns, $T_{2a} = 1.2$ ps, $d_{12a} = 10$ Debye, $N_{0a} = 18 \cdot 10^{15}$ cm^{-3}, $L_a = 0.22$ cm. Red arrow indicates the direction of pulse propagation.

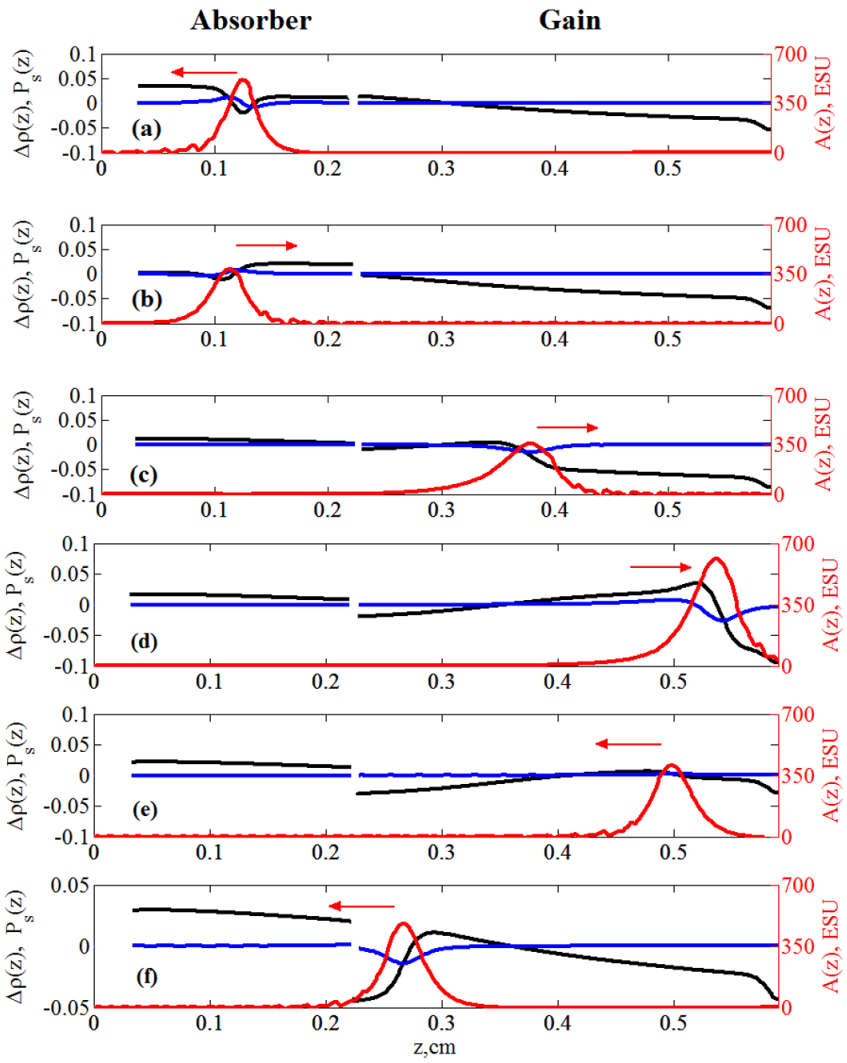

Figure 22: (a)-(f) Distribution of the electric field amplitude $A(z)$ (red line), polarization amplitude $P_s(z)$ (blue line) and population difference $\Delta\rho(z)$ (black line) in the linear cavity laser in the coherent passive mode-locking regime during a single round-trip for different positions and directions of propagation of pulse in the gain and absorbing sections. The reflectivity of the left mirror $R = 1$. Other parameters are as in Fig. 21. Red arrow indicates the direction of pulse propagation.

if the T_2 is larger or comparable with the pulse duration and cavity round-trip time. In the linear cavity laser, analogously to the ring cavity one, the pulse duration depends on the dipole moment ratio m_d. This ratio may influence also the existence of single or multiple pulses per round-trip time. Thus, the predictions provided by the McCall and Hahn diagrams are well reproduced by numerical experiments.

In summary, in this section we demonstrated a possibility of coherent mode-locking in a two-section linear cavity laser. The particular pulse regimes are quite different from the ones appearing in the ring cavity laser.

6 Conclusions

In this section we summarize the results of the present paper. We have presented a theoretical justification of the possibility of coherent passive mode-locking in a two-section laser, appearing due to the coherent character of light-matter interaction. An important feature of coherent mode-locking is the possibility to generate short optical pulses with spectral bandwidth wider than the gain bandwidth of the active medium.

Qualitative consideration of the coherent passive mode-locking based on the area theorem of McCall and Hahn and its graphical representation has been performed here. We developed a diagram technique, allowing to elucidate the resulting regime qualitatively, in particular to find stable limit cycles in the system. Examples of such stable pulsed limit cycles have been presented. It has been shown that the regime of the coherent mode-locking can occur, depending on the parameters, via self-starting, or via an injection of an external seed pulse. The parameters of the pulses depend heavily on the ratio of the transition dipole moments of the absorber and the gain media. The duration of the pulse decreases if this ratio increases. When it is smaller than 1 or more than 3, multiple pulses on a single cavity round-trip arise.

To perform numerical experiments, a model of a two-section laser has been developed, which is based on Maxwell-Bloch equations in the slowly varying envelope approximation. The results of numerical experiments have demonstrated the existence of coherent mode-locking regimes in a two-section laser with a ring or linear cavity in a wide range of parameters. The regime of coherent mode-locking can be realized in semiconductor lasers, solid-state or gas lasers. The results of the numerical simulations show also that certain amount of energy is saved in the absorber in between the pulse passages, allowing for complicated pulse-to-pulse dynamics. The scenarios of coherent mode-locking which have been considered in this paper differ from those previously proposed in the literature. In particular, to realize stable coherent mode-locking regime in a two-section laser the injection of an external seeding pulse has been shown to be unnecessary. Our numerical simulations show also that the coherent mode-locking exists in the lasers with cavities having low Q factors, unlike the earlier proposal of a soliton laser in [53].

Finally, it is to be mentioned that the effect of SIT was discovered and explained by McCall and Hahn more than 40 years ago. However, the SIT has not found up to now significant applications in photonics because of high powers and high instrumental precision needed for this technique. From the practical point of view, the incoherent mode-locking schemes have been up to now superior over coherent ones. Nevertheless we believe that implementation of the co-

herent mode-locking in two-section lasers proposed here allows to overcome the fundamental limits of the “classical” mode-locking techniques and to use such lasers as sources of ultrashort pulses with high repetition rate.

Authors are grateful to Dr. I. A. Chekhonin and Dr. A. Pimenov for helpful discussions.

References

[1] A. J. DeMaria, D. A. Stetser, and H. Heynau. Self mode-locking of lasers with saturable absorbers. *Applied Physics Letters*, 8(7):174–176, 1966.

[2] D. A. Stetser and A. J. DeMaria. Optical spectra of ultrashort optical pulses generated by mode-locked glass: Nd lasers. *Applied Physics Letters*, 9(3):118–120, 1966.

[3] W. H. Glenn, M. J. Brienza, and A. J. DeMaria. Mode locking of an organic dye laser. *Applied Physics Letters*, 12(2):54–56, 1968.

[4] T. I. Kuznetsova, V. I. Malyshev, and A. S. Markin. Self-synchronization of axial modes of a laser with saturable filters. *Soviet Physics JETP*, 25(2):286–291, 1967.

[5] H. W. Mocker and R. J. Collins. Mode competition and self-locking effects Q-switched Ruby laser. *Applied Physics Letters*, 7(10):270–273, 1965.

[6] N. G. Basov, P. G. Kriukov, V. S. Letokhov, and Yu. Senatskii. Generation and amplification of ultrashort optical pulses. *IEEE Journal of Quantum Electronics*, 4(10):606–609, 1968.

[7] N. G. Basov, P. G. Krjukov, and V. S. Letokhov. Ultra-short light pulses. *Optics Technology*, 2(3):126–131, 1970.

[8] U. Keller. Recent developments in compact ultrafast lasers. *Nature*, 424(6950):831–838, 2003.

[9] D. Bimberg, M. Grundmann, and N. N. Ledentsov. *Quantum dot heterostructures*. John Wiley Chichester, 1999.

[10] D. Bimberg. Quantum dot based nanophotonics and nanoelectronics. *Electronics Letters*, 44:168–171, 2008.

[11] E. U. Rafailov, M. A. Cataluna, and E. Avrutin. *Ultrafast Lasers Based on Quantum-dot Structures: Physics and Devices*. WILEY-VCH Verlag, 2011.

[12] E. U. Rafailov, M. A. Cataluna, and W. Sibett. Mode-locked quantum-dot lasers. *Nature Photonics*, 1:395–401, 2007.

[13] U. Keller, K. J. Weingarten, F. X. Kartner, D. Kopf, B. Braun, I. D. Jung, R. Fluck, C. Honninger, N. Matuschek, and J. Aus der Au. Semiconductor saturable absorber mirrors (SESAM's) for femtosecond to nanosecond pulse generation in solid-state lasers. *IEEE Journal of Selected Topics in Quantum Electronics*, 2(3):435–453, 1996.

[14] D. Arsenijević, M. Kleinert, and D. Bimberg. Passive mode-locking of quantum-dot lasers. *IEEE Photonics Journal*, 6:0700306, 2013.

[15] P. G. Kryukov and V. S. Letokhov. Propagation of a light pulse in a resonantly amplifying (absorbing) medium. *Physics-Uspekhi*, 12(5):641–672, 1970.

[16] L. Allen and J. H. Eberly. *Optical resonance and two-level atoms*. Wiley, New York, 1975.

[17] Ya. I. Khanin. *Fundamentals of laser dynamics*. Cambridge Int. Science Publ., 2006.

[18] P. G. Kryukov and V. S. Letokhov. Fluctuation mechanism of ultrashort pulse generation by laser with saturable absorber. *IEEE Journal of Quantum Electronics*, QE-8:766–782, 1972.

[19] V. S. Letokhov. Generation of ultrashort light pulses in a laser with a nonlinear absorber. *Sov. Phys. JETP*, 28:562, 1969.

[20] P. G. Kryukov. Ultrashort-pulse lasers. *Quantum Electronics*, 31(2):95–119, 2001.

[21] P. G. Kryukov. Continuous-wave femtosecond lasers. *Physics Uspekhi*, 183:897–916, 2013.

[22] H. Haus. Theory of mode locking with a slow saturable absorber. *IEEE Journal of Quantum Electronics*, 11(9):736–746, 1975.

[23] H. A. Haus. Theory of mode locking with a fast saturable absorber. *Journal of Applied Physics*, 46(7):3049–3058, 1975.

[24] H. A. Haus. Mode-locking of lasers. *IEEE Journal of Selected Topics in Quantum Electronics*, 6(6):1173–1185, 2000.

[25] G. H. C. New. Pulse evolution in mode-locked quasi-continuous lasers. *IEEE Journal of Quantum Electronics*, 10(2):115–124, 1974.

[26] F. X. Kartner, I. D. Jung, and U. Keller. Soliton mode-locking with saturable absorbers. *IEEE Journal of Selected Topics in Quantum Electronics*, 2(3):540–556, 1996.

[27] F. X. Kurtner, J. A. der Au, and U. Keller. Mode-locking with slow and fast saturable absorbers-What's the difference? *IEEE Journal of Selected Topics in Quantum Electronics*, 4(2):159–168, 1998.

[28] R. Paschotta and U. Keller. Passive mode locking with slow saturable absorbers. *Applied Physics B*, 73(7):653–662, 2001.

[29] A. G. Vladimirov, D. Turaev, and G. Kozyreff. Delay differential equations for mode-locked semiconductor lasers. *Optics Letters*, 29(11):1221–1223, 2004.

[30] A. G. Vladimirov and D. V. Turaev. A new model for a mode-locked semiconductor laser. *Radiophysics and Quantum Electronics*, 47(10-11):769–776, 2004.

[31] A. G. Vladimirov and D. Turaev. Model for passive mode locking in semiconductor lasers. *Physical Review A*, 72(3):033808, 2005.

[32] A. G. Vladimirov, U. Bandelow, G. Fiol, D. Arsenijević, M. Kleinert, D. Bimberg, A. Pimenov, and D. Rachinskii. Dynamical regimes in a monolithic passively mode-locked quantum dot laser. *JOSA B*, 27(10):2102–2109, 2010.

[33] D. Rachinskii A. G. Vladimirov and M. Wolfrum. *Modeling of passively mode-locked semiconductor lasers (in Nonlinear Laser Dynamics: From Quantum Dots to Cryptography)*. Wiley-VCH, 2012.

[34] N. Rebrova, G. Huyet, D. Rachinskii, and A. G. Vladimirov. Optically injected mode-locked laser. *Physical Review E*, 83:066202, 2011.

[35] G. Fiol, D. Arsenijević, D. Bimberg, A. G. Vladimirov, M. Wolfrum, E. A. Viktorov, and P. Mandel. Hybrid mode-locking in a 40 GHz monolithic quantum dot laser. *Applied Physics Letters*, 96(1):011104–011104, 2010.

[36] R. Arkhipov, A. Pimenov, M. Radziunas, D. Rachinskii, A. G. Vladimirov, D. Arsenijević, H. Schmeckebier, and D. Bimberg. Hybrid mode-locking in semiconductor lasers: simulations, analysis and experiments. *IEEE Journal of Selected Topics in Quantum Electronics*, 19:100208–1100208, 2013.

[37] C. Rulliere. *Femtosecond laser pulses*. Springer, 1998.

[38] N. G. Basov, R. V. Ambartsumyan, V. S. Zuev, P. G. Kryukov, and V. S. Letokhov. Nonlinear amplification of light pulses. *Sov. Phys. JETP*, 23(1):16–22, 1966.

[39] R. V. Ambartsumyan, N. G. Basov, V. Zuev, P. G. Kryukov, and V. S. Letokhov. Short-pulse Q-switched laser with variable pulse length. *IEEE Journal of Quantum Electronics*, 2(9):436–441, 1966.

[40] A. N. Oraevsky. Superluminal waves in amplifying media. *Physics-Uspekhi*, 41(12):1199–1209, 1998.

[41] N. N. Rozanov. Superluminal localized structures of electromagnetic radiation. *Physics-Uspekhi*, 48(2):167–171, 2005.

[42] S. L. McCall and E. L. Hahn. Self-induced transparency by pulsed coherent light. *Physical Review Letters*, 18(21):908, 1967.

[43] S. L. McCall and E. L. Hahn. Self-induced transparency. *Physical Review*, 183(2):457, 1969.

[44] I. A. Poluéktov, Yu. M. Popov, and V. S. Roitberg. Coherent effects in the propagation of ultrashort light pulses in resonant media. Part I (review). *Soviet Journal of Quantum Electronics*, 4(4):423, 1974.

[45] E. M. Belenov and P. P. Vasil'ev. Coherent effects in generation of ultrashort light pulses in a semiconductor injection laser. *Zh. Eksp. Teor. Fiz.*, 96(5):1629–1637, 1989.

[46] P. P. Vasil'ev. Role of a high gain of the medium in superradiance generation and in observation of coherent effects in semiconductor lasers. *Quantum Electronics*, 29(10):842, 1999.

[47] D. L. Boiko and P. P. Vasilev. Superradiance dynamics in semiconductor laser diode structures. *Optics Express*, 20(9):9501–9515, 2012.

[48] A. Capua, O. Karni, G. Eisenstein, and J. P. Reithmaier. Electron wavefunction probing in room-temperature semiconductors: direct observation of rabi oscillations and self-induced transparency. *arXiv preprint arXiv:1210.6803*, 2012.

[49] O. Karni, A. Capua, G. Eisenstein, V. Sichkovskyi, V. Ivanov, and J. P. Reithmaier. Rabi oscillations and self-induced transparency in InAs/InP quantum dot semiconductor optical amplifier operating at room temperature. *Optics Express*, 21(22):26786–26796, 2013.

[50] H. Choi, V. Gkortsas, L. Diehl, D. Bour, S. Corzine, J. Zhu, G. Höfler, F. Capasso, F. Kärtner, and T. B. Norris. Ultrafast Rabi flopping and coherent pulse propagation in a quantum cascade laser. *Nature Photonics*, 4(10):706–710, 2010.

[51] A. Gordon, C. Y Wang, L. Diehl, F. X. Kärtner, A. Belyanin, D. Bour, S. Corzine, G. Höfler, H. C. Liu, and H. Schneider. Multimode regimes in quantum cascade lasers: From coherent instabilities to spatial hole burning. *Physical Review A*, 77(5):053804, 2008.

[52] D. V. Novitsky. Ultrashort pulses in an inhomogeneously broadened two-level medium: soliton formation and inelastic collisions. *Journal of Physics B: Atomic, Molecular and Optical Physics*, 47(9):095401, 2014.

[53] V. V. Kozlov. Self-induced transparency soliton laser via coherent mode locking. *Physical Review A*, 56:1607–1612, 1997.

[54] V. V. Kozlov. Self-induced-transparency soliton laser. *JETP Lett.*, 69(12):906–911, 1999.

[55] C. R. Menyuk and M. A. Talukder. Self-induced transparency mode-locking of quantum cascade lasers. *Physical Review Letters*, 102(2):023903, 2009.

[56] M. A. Talukder and C. R. Menyuk. Analytical and computational study of self-induced transparency mode locking in quantum cascade lasers. *Physical Review A*, 79(6):063841, 2009.

[57] V. V. Kozlov, N. N. Rosanov, and S. Wabnitz. Obtaining single-cycle pulses from a mode-locked laser. *Physical Review A*, 84(5):053810, 2011.

[58] V. V. Kozlov and N. N. Rosanov. Single-cycle-pulse passively-mode-locked laser with inhomogeneously broadened active medium. *Physical Review A*, 87(4):043836, 2013.

[59] V. V. Kozlov and N. N. Rosanov. Numerical modeling of generation of few-cycle pulses in a mode-locked laser. *Optics and Spectroscopy*, 114(5):798–803, 2013.

[60] M. D. Crisp. Propagation of small-area pulses of coherent light through a resonant medium. *Physical Review A*, 1(6):1604, 1970.

[61] J. E. Rothenberg, D. Grischkowsky, and A. C. Balant. Observation of the formation of the zero-area pulse. *Physical Review Letters*, 53:552–555, 1984.

[62] S. A. Akhmanov and S. U. Nikitin. *Physical Optics*. Oxford University Press, 1997.

[63] A. Yariv. *Quantum Electroncs*. Wiley, New York, 1975.

[64] E. Lippert and J. D. Macomber. *Dynamics during spectroscopic transitions: basic concepts*. Springer Verlag, 1995.

[65] P. A. Apanasevich. Basics of the theory of interaction of light with matter. Minsk, Nauka i Tehnika, 1977.

[66] M. V. Arkhipov, R. M. Arkhipov, and S. A. Pulkin. Effects of inversionless lasing in two-level media from the point of view of specificities of the spatiotemporal propagation dynamics of radiation. *Optics and Spectroscopy*, 114(6):831–837, 2013.

[67] R. M. Arkhipov, M. V. Arkhipov, V. S. Egorov, I. A. Chekhonin, M. A. Chekhonin, and S. N. Bagaev. Effective excitation of polaritonic modes in optical cavity with resonant inversionless medium. *Nauchno-Tekhnicheskii Zh. Priborostroenie*, 7:42–48, 2012.

[68] P. Siddons. Light propagation through atomic vapours. *Journal of Physics B Atomic Molecular Physics*, 47(9):3001, 2014.